Review and Analysis

Harry Vereecken*
Lutz Weihermüller
François Jonard
Carsten Montzka

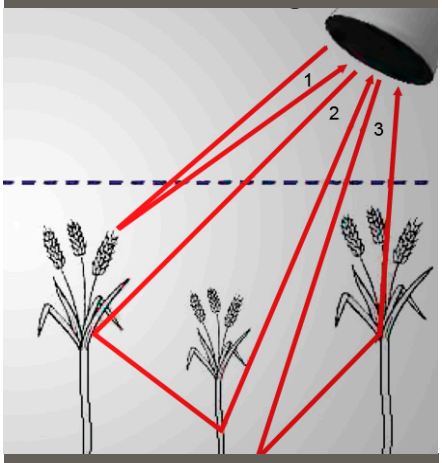

This paper reviews the value of microwave methods to characterize canopies of agricultural crops. It highlights their use in detecting water stress related phenomena and it indicates avenues for further research. Especially, the combination of microwave methods with other remote sensing methods and new crop modeling approaches seems very promising.

Harry Vereecken, Lutz Weihermüller, François Jonard, and Carsten Montzka, Agrosphere Institute IBG 3, Forschungszentrum Jülich GmbH, 52425 Jülich, Germany. *Corresponding author (h.vereecken@fz-juelich.de).

Vadose Zone J.
doi:10.2136/vzj2011.0138ra
Received 25 Oct. 2011.

Characterization of Crop Canopies and Water Stress Related Phenomena using Microwave Remote Sensing Methods: A Review

In this paper we reviewed the use of microwave remote sensing methods for characterizing crop canopies and vegetation water stress related phenomena. Our analysis includes both active and passive systems that are ground-based, airborne, or spaceborne. Most of the published results that have examined crop canopy characterization and water stress have used active microwave systems. In general, quantifying the effect of dynamic vegetation properties, and water stress related processes in particular, on the measured microwave signals can still benefit from improved models and more observational data. Integrated data sets providing information on both soil status and plant status are lacking, which has hampered the development and validation of mathematical models. There is a need to link three-dimensional functional, structural crop models with radiative transfer models to better understand the effect of environmental and related physiological processes on microwave signals and to better quantify the impact of water stress on microwave signals. Such modeling approaches should incorporate both passive and active microwave methods. Studies that combine different sensor technologies that cover the full spectral range from optical to microwave have the potential to move forward our knowledge of the status of crop canopies and particularly water related stress phenomena. Assimilation of remotely sensed properties, such as backscattering coefficient or brightness temperature, in terms of estimating biophysical crop properties using mathematical models is also an unexplored avenue.

Abbreviations: HH, copolarized horizontal transmit, horizontal receive [polarization]; IHS, intensity–hue–saturation; IR, infrared; LAI, leaf area index; MPDI, Microwave Polarization Difference Index; MPDT, Microwave Polarization Difference Temperatures; MVIs, Microwave Vegetation Indices; NDVI, Normalized Difference Vegetation Index; PCA, principal component analysis; SAR, synthetic aperture radar; VOD, vegetation optical depth; VV, copolarized vertical transmit, vertical receive [polarization].

Over the last three decades there has been a growing awareness of the importance of land surface processes and their value in predicting climate change and its subsequent impact on the terrestrial system, managing water resources, and predicting and monitoring floods and droughts. Remote sensing from Earth observation platforms has played a key role by providing valuable data to the scientific community, from local to global scales and at different time scales. Given the importance of the land surface for terrestrial processes and for agricultural activity, the characterization and monitoring of vegetation and crops has been an important focus area in remote sensing of the Earth surface. Historically, remote sensing of vegetation has focused primarily on the use of spectral measurements in the visible, near infrared, and shortwave infrared region of the spectrum. This region is important because the reflectance measurements are governed primarily by the scattering and absorption characteristics of the leaf internal structure and biochemical constituents. Overviews of the satellite-based results can be found in Lu (2006) for biomass estimation, Zheng and Moskal (2009) for leaf area index (LAI) retrieval, Govender et al. (2009) for multispectral detection of plant water stress, and Pinter et al. (2003) for crop management.

During the last decade, satellite and spaceborne synthetic aperture radar (SAR) systems (i.e., ALOS PALSAR, RADARSAT-1 & 2, ERS-1 & 2, ENVISAT ASAR, SIR-C/X SAR, TerraSAR-X) and microwave radiometers (i.e., AQUA AMSR-E, Coriolis WindSAT, SMOS MIRAS) have been available. (See the Appendix for a list of remote sensing system acronyms.) A list of spaceborne microwave sensors is given in Table 1 and a list of microwave frequency bands is given in Table 2. In the near future combined active and passive systems, such as AQUARIUS (launched in June 2011) and SMAP (planned launch in November 2014), will offer new opportunities in microwave remote sensing. Passive and

Table 1. List of spaceborne microwave sensors.

Name	Platform	Frequency	Spatial resolution	Temporal resolution	Active/passive
		GHz		d	
AMSR-E	AQUA	6.925, 10.65, 18.7, 23.8, 36.5, 89.0	56, 38, 21, 24, 12, 5.4 km	1	passive
ASCAT	MetOp	5.255	25 to 50 km	2	active
PALSAR	ALOS	1.27	9 to 157 m	46	active
AQUARIUS	AQUARIUS/SAC-D	1.413 (passive), 1.26 (active)	76 to 156 km	7	active and passive
ASAR	ENVISAT	5.331	30 to 1000 m	5	active
COSMO-SkyMed	COSMO-SkyMed	9.6	1 to 100 m	0.5–16	active
ERS-SAR	ERS-1 & ERS-2	5.3	30 m	3, 35, 176	active
JERS-1-SAR	JERS-1	1.3	18 m	44	active
RADARSAT 1 & RADARSAT 2	RADARSAT 1 & RADARSAT 2	5.405	10 m	24	active
SIR-A	Space Shuttle	1.28	40 m	– †	active
SIR-C/X	Space Shuttle	1.25, 5.3, 9.6	10 to 30 m	– †	active
SMAP	SMAP	1.41 (passive), 1.26 (active)	40 km (passive), 1 to 3 km (active)	2–3	active and passive
MIRAS	SMOS	1.4	35 to 60 km	3	passive
SSM/I	SSM/I	19.35, 22.2, 37.0, 85.5	13 to 69 km	0.5	passive
SeaWinds	Quickscat	13.4	25 km	1	active
Tandem-L	Tandem-L	1.2	3 to 20 m	8	active
TanDEM-X	TanDEM-X	9.65	1 to 18 m	2–4	active
TerraSAR-X	TerraSAR-X	9.65	1 to 18 m	2–4	active
WindSAT	Coriolis	6.8, 10.7, 18.7, 23.8, 37.0	8 to 71 km	8	passive

† A temporal resolution is not given because the missions took several days. SIR-A was a mission from 12 to 14 Nov. 1981; SIR-C/X was a mission from 9 to 20 Apr. 1994 and from 30 Sept. to 11 Oct. 1994.

active measurements in the microwave region of the spectrum have mainly been used to characterize biophysical parameters of the plant canopy, such as shape, size, and distribution of plant elements, water content, height of the vegetation, LAI, aboveground biomass, and number of plants (Chukhlantsev et al., 2003; Della Vecchia et al., 2007; Moran et al., 1997; Paloscia and Pampaloni, 1988). In addition, passive microwave methods at low frequencies (X, C, and L bands) have typically been used to detect bare or vegetated soil surface moisture content (Calvet et al., 2011; Guglielmetti et al., 2008; Jackson and Schmugge, 1989; Jackson et al., 1982; Jonard et al., 2011; Njoku and Entekhabi, 1996; Schmugge et al., 1974; Wigneron et al., 2003). Additionally, low frequency active systems have been used to study the role of vegetation on land surface properties. The effect of vegetation on the recovery of soil moisture was studied by Mätzler (1990), Serbin and Or (2005), and Joseph et al. (2010, 2008). O'Neill et al. (1996) used both active and passive microwave sensors for soil moisture estimation through vegetation. Vegetation transmissivity and scattering were characterized by using L-band radar data. The vegetation parameters were then used for soil moisture retrieval based on a radiative transfer approach utilizing passive microwave data. However, limited attention has been given to the use of microwave methods to detect water stress in agricultural canopies despite the advantages of these methods

Table 2. Standard IEEE microwave frequencies and nomenclature.

Band designator	Frequency	Wavelength in free space
	GHz	cm
L	1–2	30–15
S	2–4	15–7.5
C	4–8	7.5–3.8
X	8–12	3.8–2.5
Ku	12–18	2.5–1.7
K	18–27	1.7–1.1
Ka	27–40	1.1–0.75
V	40–75	0.75–0.40
W	75–110	0.40–0.27

compared to optical, and infrared (IR) multi- or hyperspectral sensors (Detar et al., 2006, and references therein). These include the ability of providing time critical remotely sensed observations, such as at night or when cloud cover is present (McNairn and Brisco, 2004) and the ability to sense the entire canopy as opposed to just the leaves. Ferrazzoli (2002) briefly reviewed the use of SAR for agricultural purposes. In addition to describing the historical evolution from ground-based measurements, to

airborne measurements, and finally satellite platforms, Ferrazzoli (2002) addressed and discussed the identification of useful radar configurations and the development of relationships between backscattering and variables for seven selected crops.

Despite the extensive body of literature available on the subject of remote sensing and vegetation, no attempt has been made at in depth evaluation and analysis of the use of active and passive microwave methods to characterize crop canopies, specifically in relation to stress phenomena. This review has three main objectives:

1. to review the use of microwave methods to characterize crop canopies with specific attention to stress-related properties such as vegetation water content and leaf water potential;
2. to analyze the effect of confounding factors on the retrieval of drought conditions or water stress in crop canopies;
3. to formulate future avenues of research related to water stress recognition in vegetation using microwave methods.

The paper is organized into eight sections. In the second section, we will present an overview of the theory and models that were developed to interpret signal propagation of microwave systems (passive and active) in aboveground agricultural vegetation properties. The third section addresses the characterization of crop canopies using ground-based measurements with specific attention to diurnal and seasonal dynamics of backscattering in canopies. The fourth section deals mainly with the characterization of crop canopies from remote sensing observations. In the fifth section, we discuss the relationship between dielectric properties of the vegetation and soil–plant water relationships, whereby these relationships are essential for the interpretation of the diurnal and seasonal changes in emissivity and backscattering. The sixth section discusses the factors controlling microwave signals obtained from crop canopies with a specific focus on water stress phenomena. Finally, we conclude this review with the topic of multisensor measurements and an outlook section presenting conclusions and avenues for further research needs.

Measurements Principles and General Modeling Approaches

This section provides a general overview of the measurement principles of passive and active systems and a brief description of electromagnetic wave propagation, attenuation, and scattering in vegetation canopies. Specific attention will be given to models specifically designed to predict emission or backscattered signals from crop canopies. Only a brief overview of the theory and the various models is provided. For more detailed information the reader will be referred to the original citations. In the presentation, we make a distinction between passive and active systems, as each system measures different properties of the canopy. Passive microwave radiometers provide the brightness temperature, T_B, of the surface, whereas active radar systems measure the backscattering coefficient, σ^0.

Passive Systems

For land surfaces, low frequency passive microwave radiometry can be used as an indirect method to measure the complex dielectric permittivity $\varepsilon = \varepsilon' + i\varepsilon''$ of a bare soil, which can be used as a proxy for the estimation of the soil moisture content (Hong and Shin, 2011; Hornbuckle et al., 2003; Saleh et al., 2007; Schneeberger et al., 2004; Wigneron et al., 1995, among many others). The determination of the permittivity, ε, is typically based on the measurement of thermal radiance emitted from the Earth surface in a given frequency band (Njoku and Entekhabi, 1996). At specific frequency, the intensity of the received radiation (thermal emission) is proportional to the thermodynamic temperature T_s [K] and the emissivity e_s of the soil, which can be expressed by the Rayleigh–Jeans approximation of Planck's Law. According to this equation, the radiance is proportional to the physical temperature of the object, and therefore, denoted as brightness temperature, T_B [K] (Njoku and Entekhabi, 1996; Wigneron et al., 2001). As a consequence, the brightness temperature of a soil surface observed for example by a radiometer operating at the L band can then be expressed as (Jackson, 1993; Wigneron et al., 2001):

$$T_{B,p} = e_{s,p} T_s + (1 - e_{s,p}) T_{sky} \quad [1]$$

where e_s is the surface emissivity, T_{sky} [K] is the sky radiometric temperature calculated following Pellarin et al. (2003), T_s [K] is the effective physical temperature of the soil, and p refers to the polarization (horizontal or vertical). However, in the presence of vegetation Eq. [1] is no longer applicable because absorption, emission, and scattering by the vegetation canopy need to be considered in the formulation of the radiative transfer model (see also Fig. 1). Therefore, T_B for one polarization of a soil–vegetation system can be expressed by:

$$T_B = T_v(1 - r_v - \gamma) + e_s T_s \gamma + T_v(1 - r_v - \gamma)(1 - e_s)\gamma \quad [2]$$

where T_v is the vegetation temperature [K], r_v is the vegetation canopy reflectivity, and γ is the transmissivity of the vegetation canopy (Chukhlantsev et al., 2003).

At low frequencies (L band) and for low vegetation, a zero-order solution of radiative transfer equation, called Tau–Omega model, can be used and is expressed by:

$$T_{B,p} = (1 - \omega_p)(1 - \gamma_p)(1 + \gamma_p r_{s,p}) T_v + (1 - r_{s,p})\gamma_p T_s \quad [3]$$

where r_s is the soil reflectivity and ω the single scattering albedo. The attenuation in the vegetation layer as described by the vegetation attenuation factor γ (or vegetation transmissivity) can be defined in terms of the optical depth (τ) and incidence angle (θ, the angle between a ray incident on a surface and the line perpendicular to the surface at the point of incidence) (Wigneron et al., 2007) by:

$$\gamma_p = \exp(-\tau_p/\cos\theta) \quad [4]$$

Jackson and O'Neill (1990) showed that a linear relationship between the optical depth (τ) and the vegetation water content (VWC [kg m^{-2}]) exists:

$$\tau_p = b_p \mathrm{VWC} \quad [5]$$

where b is a regression coefficient that is frequency and polarization dependent and characteristic for the type of canopy (Jackson and Schmugge, 1991; Van de Griend and Wigneron, 2004).

In general, the Tau–Omega model is a good approximation at low frequencies such as L band and has been intensively used to model microwave emissions from uniformly vegetated land surface at this frequency (Hornbuckle et al., 2003; Joseph et al., 2010; O'Neill et al., 1996; Wigneron et al., 2004). Within the SMOS and SMAP communities, a modified version of the Tau–Omega model is used and is called the L-band Microwave Emission of the Biosphere (L-MEB) model (Wigneron et al., 2007).

Only a few physically based radiative transfer models have been developed that account for the vegetation explicitly. These models are mainly used to correct for the vegetation influence to improve soil moisture observations in forest stands (Della Vecchia et al., 2006; Ferrazzoli and Guerriero, 1996). Only a few approaches were made to physically model agricultural crops, such as the explicit model presented by Schwank et al. (2005), who showed that changes in the plant geometry (here induced by a hail storm over clover grass) will greatly influence measured brightness temperatures.

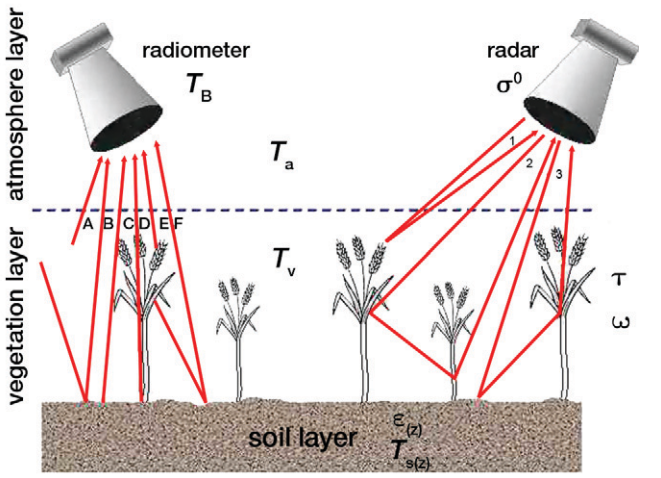

Fig. 1. Schematic illustration of the different components of the passive and active signals measured by radiometer and radar, respectively. T_B is the brightness temperature measured by the radiometer, σ^0 is the backscattering coefficient measured by the radar, T_a is the temperature profile of the atmosphere layer, T_v is the temperature profile of the vegetation layer, τ is the vegetation optical depth, ω is the single scattering albedo of the vegetation layer, $T_{s(z)}$ is the temperature profile in the soil, and $\varepsilon_{(z)}$ is the dielectric permittivity profile in the soil. Also shown are the signal emitted by the radar and reflected on the vegetation canopy (1), the radar signal reflected by the vegetation stems to the radar antenna (2), the radar signal reflected by the soil surface and then the vegetation to the radar antenna (3), the passive microwave signal emitted from the atmosphere (A), the microwave emission from the atmosphere and reflected by the soil to the radiometer antenna (B), the microwave emission from the soil (C), the microwave emission from soil transmitted to the radiometer antenna through the vegetation layer (D), the microwave emission from the vegetation canopy (E), and the microwave emission from the vegetation canopy reflected by the soil to the radiometer antenna (F).

Active Systems

Active systems such as radars or scatterometers are typically used to define the backscattering coefficient of the land surface. The backscattering coefficient, which is the effective scattering area of the target per unit area, is directly proportional to the ratio of the backscattered to the emitted energy. For a soil–vegetation system (Fig. 1) the backscattering coefficient is generally expressed as:

$$\sigma^0 = \sigma_s^0\gamma^2 + \sigma_v^0(1-\gamma^2) + \sigma_{sv}^0 \quad [6]$$

where σ_s^0 and σ_v^0 are the backscattering coefficients of the soil and vegetation canopy, respectively, and σ_{sv}^0 is the backscattering coefficient of the vegetation layer including the reflection from the soil and the attenuation by the vegetation (Chukhlantsev et al., 2003).

In the early years of radar application over vegetation, empirical models were developed using regression analysis of the radar backscattering on plant moisture, plant height, and the moisture content of the underlying soil (Bush and Ulaby, 1976; Ulaby and Bush, 1976a,b). However, no knowledge about the physical processes was assumed or incorporated into the empirical models.

During the last decades physically based models were developed to describe the propagation, scattering, and attenuation of the electromagnetic waves in the vegetation layer. A detailed treatment and overview of models and microwave sensing theories is given by Ulaby et al. (1986) and Fung (1994). Chukhlantsev et al. (2003) distinguished two fundamentally different types of model approaches: (i) the continuous layer models with a randomly distributed dielectric constant (the so called cloud models) and (ii) models assuming a set of randomly distributed lossy scatters representing the different constituents of the vegetation, such as leaves, stalks, branches, and trunks.

Attema and Ulaby (1978) developed a cloud model for radar backscattering from vegetation. In this model, it is assumed that the vegetation is mainly composed of water that is surrounded by a large air volume. Therefore, the vegetation water can be represented by a water cloud whose water droplets are held in place by the

vegetation. The model is based on the assumption that the canopy "cloud" contains identical water droplets that are randomly distributed within the canopy. The model was successfully applied by Paris (1986), Prevot et al. (1993), Taconet et al. (1994), Wigneron et al. (2002), Maity et al. (2004), and Serbin and Or (2005) for different applications and crop stands. It has to be noted that various authors modified the "simple cloud model" to increase the complexity and as a consequence the overall performance of the model (Paris, 1986). Ulaby et al. (1990) developed the Michigan Microwave Canopy scattering model for forest systems, which is a widely used model in active microwave remote sensing. This model was successfully adapted to agricultural crops by Touré et al. (1994).

Eom and Fung (1984) developed a scatter model based on the matrix doubling method for volume scattering and the Kirchhoff method for rough surface scattering. They assumed that the scattering from the vegetation is dominated by the leaves, and therefore single leaves can be modeled by thin dielectric discs. Finally, the vegetation layer was modeled as a layer of leaves above an irregular soil surface. Additionally, the phase function for a single leaf was computed by approximating an integral equation for the electric field. To obtain closed form equations strong assumptions have to be made. These include: (i) that the field variation across the thickness of the leaf is negligible and (ii) that the phase change across the surface of the leaf can be accounted for by integrating the static field. Thus, the model is a static approximation generalized to include phase changes across the leaf surface. Finally, the closed form solution for the scattering coefficient contains three terms. One term represents volume scattering, another term represents ground-surface scattering attenuated by the vegetation, and the last term accounts for surface–volume interactions.

Further research included various modifications and improvements to increase the physical representation of the model for different crops and frequencies. For example, Della Vecchia et al. (2004) modeled the radar backscattering from a canopy with leaves described as curved rectangular dielectric sheets based on the Tor Vergata model (Bracaglia et al., 1995). Stiles and Sarabandi (2000) developed a fully phase coherent scattering models for grassland, and Marliani et al. (2002) for crops such as sunflower (*Helianthus annuus* L.) and wheat (*Triticum aestivum* L.).

For fully developed crops the canopy may become dense, and multiple scatter effects may occur (Picard et al., 2003), which requires an improved description of the radiative transfer by taking into account higher order effects (Ferrazzoli and Guerriero, 1996). Additionally, resolving radiative interactions with complex multilayer objects often requires an explicit three-dimensional modeling of radiation pathways via ray tracing methods (Battaglia et al., 2006).

Characterization of Crop Canopies Using Ground-Based Measurements

Combined Crop and Microwave Measurements

To gain information about the biophysical crop parameters, three different types of retrieval algorithms are in use either for passive or active systems. The first type is based on empirical functions (e.g., regression equations) between the quantity measured (emission or backscattering coefficient) and the biophysical parameter investigated, whereby these empirical equations are often only valid for the test site, the region, or the crop investigated. The second type of retrieving algorithms is based on neural network predictions. In this approach it is necessary to train the corresponding neural network by statistically representative sampling. In many cases such training is not always feasible. The third type of algorithms is based on the inversion of radiation models, and it is most widely used. In this approach, the models relate the radiation parameters to environmental parameters, such as the vegetation canopy (Chukhlantsev et al., 2003). In the following we give a literature overview of studies that provide both microwave data obtained from ground-based systems and crop data. Additionally, we organized the discussion along the two major measurement systems.

Active Systems

Table 3 gives an overview of literature studies that provide information on ground-based radar backscattering measurements, crop canopy properties, and soil moisture content. This table also provides information on the use of air- and spaceborne microwave platforms that are discussed below in "Characterization of Crop Canopies using Air- and Spaceborne Remote Sensing." In general, our analysis of literature dealing with crop characterization and stress detection showed that most studies used active systems. This is especially the case for the analysis of diurnal and seasonal dynamics observed in crop canopies, as discussed in "Diurnal Dynamics of Backscattering in Crop Canopies and Seasonal Dynamics of Backscattering in Crop Canopies" below. Although active and passive systems have both their advantages and disadvantages, active radar systems on air- and spaceborne platforms provide higher spatial resolution than passive systems. One reason could be that mapping and characterizing canopies as well as detecting water stress phenomena typically requires a high spatial resolution due to the inherent heterogeneity of land cover. In the case of soil moisture mapping this picture might look different. Due to the limited number of studies using passive systems, we refrained from including an explicit table in the text but referred to the relevant references in two separate subsections (see "Passive Systems").

The majority of the experiments using active systems were conducted on cereals such as wheat and sorghum [*Sorghum bicolor* (L.) Moench], corn (*Zea mays* L.), soybean [*Glycine max* (L.) Merr.], alfalfa (*Medicago sativa* L.), ladyfinger (*Musa acuminata* Colla),

Table 3. Overview of literature studies providing information on microwave radar measurements over crops and crop characteristics.

	Crops		Radar measurements			Crop and soil measurements†								
Authors	Crop type	Scale	Platform name, frequency	Polarization, incidence angle	Duration, number	LAI	NP	BM	PH	LS	LT	WP	VWC	SMC
Ground-based radar														
Ulaby and Batlivala (1976)	Sorghum	Field (irrigation)	2–8 GHz	HH, VV	27 June–7 July 1974 (diurnal meas.)	–	–	–	+	–	–	–	–	+
				0–50°										
Brakke et al. (1981)	Wheat, corn, sorghum	Field	8.6, 13.0, 17.0, 35.6 GHz	HH, HV, VV	4 weekly scans (1979)	+	+	+	+	–	–	+	+	+
				30, 50, 70°										
Ulaby and Jedlicka (1984)	Corn, sorghum, wheat	Field	8.6, 13.0, 17.0, 35.6 GHz	HH, HV, VV	7 meas. (1979) and 23 meas. (1980)	+	+	+	+	–	–	–	+	+
				30, 50, 70°										
Wu et al. (1985a)	Winter wheat, soybean, corn	Field (defoliation)	X band (10 GHz)	VV	Wheat: 2 d	–	–	–	–	–	–	–	–	–
				30, 50°	Soybean: 2 d									
					Corn: 3 d									
Paris (1986)	Corn	Field	17 GHz	HH, VV	Growing season	+	–	+	–	–	–	–	+	+
				50°	(25 meas.)									
Brisco et al. (1990)	Wheat	Field	L, C, and K band (1.5, 5.17, 12.8 GHz)	HH, VV, HV 20–60°	3 times 24–30 h (Aug. 1987, June and July 1988)	–	–	–	+	–	–	–	+	+
Bouman and Van Kasteren (1990a)	Sugarbeet, potato	Field	X band (9.5 GHz)	VV, HH, HV, VH, 10–80°	1975–1981	+	+	+	+	+	+	–	+	+
Bouman and Van Kasteren (1990b)	Wheat, barley, oat	Field	X band (9.5 GHz)	VV, HH	1975–1981	–	–	–	–	–	–	–	–	–
				10–80°										
Bouman (1991)	Sugarbeet, potato, wheat, barley	Field	X band (9.5 GHz)	VV, HH, HV, VH,	1975–1981	+	+	+	+	+	+	–	+	+
				10–80°										
Forster et al. (1991)	Tomato	Pot (water-stressed)	X band	HH	12 d	–	–	–	–	–	–	+	+	–
				25°	(daily)									
Wegmüller (1993)	Corn, wheat, sugarbeet, potato, grass, canola, oat, rye	Field	RASAM	HH, VV,VH	1984–1989	+	+	+	+	+	+	–	+	+
			3–11 GHz	0–70°										
Colpitts and Coleman (1997)	Potato	Pot (water-stressed)	L, C, and K band (45 MHz-26.5 GHz)	0°	–	–	–	–	–	–	–	+	+	–
Chauhan (1997)	Alfalfa	Field	COMRAD L band (1.6 GHz)	HH, VV 10–60°	5 d (June 1992)	–	+	–	+	+	+	–	+	+

Table 3. Continued.

Authors	Crops		Radar measurements			Crop and soil measurements†								
	Crop type	Scale	Platform name, frequency	Polarization, incidence angle	Duration, number	LAI	NP	BM	PH	LS	LT	WP	VWC	SMC
Stiles and Sarabandi (2000)	Wheat	Field	L, C, X band (1.25, 5.3, 9.5 GHz)	VV, HH, HV	–	+	+	+	+	+	+	–	+	+
				20–70°										
Mattia et al. (2003)	Wheat	Field	C band (5.3 GHz)	HH, VV	Mar.–June 2001	–	+	+	+	+	–	–	–	+
				23–60°	(8 meas.)									
Brown et al. (2003)	Wheat	Laboratory and field	GB-SAR	VV, HH, VH	June-July 1999	+	+	+	+	+	–	–	+	+
			C, X band (lab.)	20–50°										
			L, X band (field)											
Picard et al. (2003)	Wheat	Field	C band	HH, VV,	9 d, Mar.–June 2001	–	+	+	+	–	–	–	+	+
				23–60°										
Del Frate et al. (2004)	Wheat	Field	RASAM	VV, HH	1988	–	–	+	+	–	–	–	–	+
			3.1–10.2 GHz	10–70°										
Serbin and Or (2005)	Wheat	Greenhouse (irrigation)	1 GHz	0°	9 Mar.–7 May 2002 (every 30 min)	+	+	+	+	–	–	–	+	+
Serbin and Or (2005)	Corn	Field	1 GHz	VV	–	+	+	+	+	–	–	–	+	+
				7.5, 17°										
Gómez-Dans et al. (2006)	Wheat	Laboratory	GB-SAR	HH, VV, HV	June–July 1999	–	–	–	+	–	–	–	–	–
			C band (5.44 GHz)	35–55°										
Singh (2006)	Soybean	Field (irrigation)	X band (9.5 GHz)	HH, VV	90 d	+	+	+	+	–	–	–	–	+
				20–70°	(every 10 d)									
Della Vecchia et al. (2006)	Maize	Field	RASAM	HH, VV, HV, VH	May–Oct. 1988	+	+	+	+	+	+	–	+	+
			C band	30°										
Della Vecchia et al. (2008)	Maize	Field	RASAM	HH, VV, HV	May–Oct. 1988	–	–	+	+	–	–	–	+	+
			2.5–10.2 GHz	20–50°	(23 meas. days)									
Joseph et al. (2008)	Corn	Field	COMRAD	HH, VV	Apr.–Oct. 2002	–	–	+	+	–	–	–	+	+
			L band (1.6 GHz)	15, 35, 55°	(1 per week)									
Prasad (2009)	Ladyfinger	Field	X band (9.9 GHz)	HH, VV	90 d	+	–	+	+	–	–	–	–	+
				20–70°	(10 per day)									
Joseph et al. (2010)	Corn	Field	COMRAD	HH, VV	Apr.–Oct. 2002	–	–	+	+	–	–	–	+	+
			C, L band (4.5, 1.6 GHz)	15, 35, 55°	(1 per week)									

Table 3. Continued.

Authors	Crops		Radar measurements			Crop and soil measurements†								
	Crop type	Scale	Platform name, frequency	Polarization, incidence angle	Duration, number	LAI	NP	BM	PH	LS	LT	WP	VWC	SMC
Air- and spaceborne radar														
Prévot et al. (1993)	Wheat	Field	ERASME (airb.)	C band	1988 (4 d)	+	–	+	+	–	–	–	+	+
			C, X band (5.35, 9.65 GHz)	HH, 15–30°										
				X band										
				VV, 30–45°										
Bouman and Hoekman (1993)	Sugar-beet, potato, winter wheat	Field	DUTSCAT (airb.)	HH, VV	1988 (7 d)	+	–	+	+	+	+	–	+	+
			L, C, X, Ku band (1.2, 3.2, 5.3, 9.6, 13.7, 17.25 GHz)	10–60°										
Taconet et al. (1994)	Wheat	Field	ERASME (airb.)	HH, VV	16 June–28 July 1988 (4 dates)	+	–	+	+	–	–	–	+	+
			C, X band (5.35, 9.65 GHz)	20–40°	21 Mar.–18 July 1989 (5 dates)									
Bouman et al. (1999)	Sugar beet, potato, winter wheat	Field	ERS/SAR (spaceb.)	VV	1992–1994	+	–	–	–	–	–	–		+
			C band (5.3 GHz)	23°										
Cookmartin et al. (2000)	Wheat, barley, oilseed rape	Field	ERS-2/SAR	VV	1997 (7 d)	+	+	–	+	+	+	–	+	+
			C band (5.3 GHz)	23°										
Macelloni et al. (2001)	Wheat, sunflower	Field	AIRSAR (airb.)	AIRSAR:	Summer 1991 (AIRSAR)	+	+	+	+	+	+	–	+	+
			P, L, C band	HH, VV, HV, VH	Summer 1994 (EMISAR)									
			EMISAR (airb.)	20, 35, 50°	April, October 1994 (SIR-C/X-SAR)									
			L, C band	EMISAR:	ERS-1/2 and JERS-1 (1992–1994)									
			SIR-C/X-SAR (spaceb.)	HH, VV, HV										
			L, C/X band	45°- 50°										
			ERS-1/2/SAR (spaceb.)	SIR-C/X-SAR:										
			C band	HH, VV, HV, VH/VV										
			JERS-1/SAR (spaceb.)	23–55°										
			L band	ERS-1/2: VV, 23°										
				JERS-1: HH, 35°										
Wigneron et al. (2002)	Sunflower	Field	ERASME (airb.)	VV	Oct. 1996–Nov. 1997	+	–	+	+	–	–	–	–	+

Table 3. Continued.

Authors	Crops		Radar measurements			Crop and soil measurements†								
	Crop type	Scale	Platform name, frequency	Polarization, incidence angle	Duration, number	LAI	NP	BM	PH	LS	LT	WP	VWC	SMC
			ERS-2/SAR (spaceb.)	20–23°										
			C band											
Blaes and Defourny (2003)	Winter wheat, sugar-beet, potato, maize	Field	ERS-1/2/SAR (spaceb.)	VV	Mar. –July 1996	+	–	–	+	–	–	–	–	+
			C band	23°										
Picard et al. (2003)	Wheat	Field	ERS/SAR (spaceb.)	VV	4 d, Mar.–June 2000	–	+	+	+	–	–	–	+	+
			C band	23°										
Maity et al. (2004)	Cotton	Field	RADARSAT/SAR	HH	2001 (3 d)	+	+	–	+	–	–	–	–	+
			C band (5.3 GHz)	36–42°										
Del Frate et al. (2004)	Wheat	Field	ERS-2/SAR (spaceb.)	VV	1997	+	–	+	–	+	–	–	+	+
			C band	23°										
Blaes et al. (2006)	Corn	Field	ENVISAT/SAR (spaceb.)	HH, VV	Jan.–Sept. 2003	+	+	+	+	+	+	–	+	+
			ERS-2/SAR (spaceb.)	15–45°										
			RADARSAT/ SAR (spaceb.)											
			C band											
Liu et al. (2006)	Winter wheat	Field	ENVISAT/ASAR (spaceb.)	HH, VV	2004 (Mar.–June)	+	–	+	–	–	–	–	+	+
			C band	42.5–45.2°										
Della Vecchia et al. (2006)	Wheat, maize	Field	ERS-2/SAR (spaceb.)	ERS:	2001, 2003	+	+	+	+	+	+	–	+	+
			ENVISAT (spaceb.)	VV, 20–25°										
			C band	ENVISAT:										
				VV, 20–42°										
Baghdadi et al. (2009)	Sugarcane	Field	TERRASAR-X (spaceb.)	TerraSAR:	2006–2008	–	–	–	+	–	–	–	–	–
			X band (9.65 GHz)	HH, 39, 53°										
			ENVISAT/ASAR (spaceb.)	ENVISAT:										
			C band	VV, HH, HV, 18–44°										
			PALSAR/ALOS	PALSAR:										
			(spaceb.)	HH, HV,										
			L band (1.27 GHz)	36–43°										

† +, measurement performed; –, no measurement performed; LAI, leaf area index; NP, number of plants; BM, vegetation biomass; PH, plant height; LS, leaf size; LT, leaf thickness; WP, water potential; VWC, vegetation water content; SMC, soil moisture content.

and tomato (*Solanum lycopersicum* L.) with frequencies ranging from L to X band. Most experiments were performed under field conditions with natural rainfall or eventually irrigation. Typical biophysical parameters that were measured include LAI, biomass of the whole plant and its components, crop height, vegetation stage, vegetation water content, and soil moisture. In the 1970s, Ulaby and Bush (1976b) used a scatterometer in the frequency range of 8 to 18 GHz to monitor corn growth for a 4-mo period. The authors found a good correlation between normalized plant water content (i.e., the ratio of mass of water in the plant to plant height) and the radar backscattering coefficient at incidence angles of 40° or more. Higher frequencies typically showed better correlations. Bush and Ulaby (1976) used the same setup to analyze the backscattering from alfalfa. They found that, at nadir, the backscattering coefficient was dependent on variations in plant height and soil moisture content. Ulaby and Wilson (1985) used L-, C-, and X-band radars mounted on a boom truck to investigate canopy attenuation of winter wheat and soybeans. Attenuation data were acquired at 1.55, 4.75, and 10.2 GHz for copolarized horizontal transmit, horizontal receive (HH) and copolarized vertical transmit, vertical receive (VV) polarization at incidence angles of 20 and 50°. The authors found that vegetation canopies are highly nonuniform and anisotropic at microwave frequencies. They also observed large differences between the HH and VV polarization measurements of canopy attenuation, which indicated that the relative importance of ground emission and backscattering was polarization dependent. Recently, Prasad (2009) showed that the angular variation of scattering coefficient at the X band for the crop ladyfinger decreases as the plant grows since the effects of soil was masked by developing vegetation. The author also observed that scattering coefficients increased with LAI both for VV and HH polarization and that LAI and biomass are highly correlated with backscattering (more than for plant height). As already observed by Ulaby and Bush (1976b) for a corn crop, the author also noticed that at the X band, the effect of crop covered soil moisture in the retrieval of crop variables could be neglected at incidence angle of about 45° or higher.

In general, no specific attention was paid in determining parameters or variables that provide information on the water stress status of the canopy. Typical indicators, such as soil water potential, leaf water potential, or chlorophyll content, have only been measured sporadically. The study of Singh et al. (2003) is the only one available in literature that provides information between chlorophyll content of the leaves and backscattering measured in the X band. The wheat chlorophyll was shown to be sensitive to the radar backscattering coefficient at 40° incidence angle, and this sensitivity was higher for VV than for HH polarization. Forster et al. (1991) observed changes in X-band radar backscattering in water-stressed tomato canopies over several days. The dynamics in radar backscattering were correlated to the changes in leaf water potential observed during the recovery of the plant after wilting. Colpitts and Coleman (1997) also determined leaf water potential to identify the water status of the potato (*Solanum tuberosum* L.) canopy and leaves in combination with diurnal measurements of backscattering.

Passive Systems

For passive systems the vegetation cover attenuates soil emission and adds its own contribution to the emitted radiation, whereby the contribution of the vegetation depends on the vegetation characteristics (density and vegetation water content) and the frequency used for observation. For frequencies ranging between 1 and 5 GHz, the vegetation is semitransparent, and therefore, its influence on the soil moisture retrieval is reduced (Guglielmetti et al., 2007; Wigneron et al., 1995).

Numerous studies have shown the potential of passive microwave radiometers to estimate soil moisture and vegetation biomass (Jackson and Schmugge, 1989; Wegmüller, 1993, among others). Soil moisture content and vegetation biomass were both retrieved over the growing season of soybean and wheat by Wigneron et al. (1995). The authors used multiple angle measurements of brightness temperature at L and C band and found that the retrieval process was more accurate and stable if both bands are analyzed simultaneously and if multiple observation angles (10–40°) were included in the analysis. Liu et al. (2002) investigated the retrieval of vegetation water content from the combined brightness temperatures at the X and L bands using the crane-based PORTOS radiometer and an error propagation learning back propagation neural network. The combined use of both frequencies significantly outperformed the accuracy of single channel analyses.

So far our knowledge about the sensitivity of the microwave measurements to the plant water stress is very limited. Paloscia and Pampaloni (1984) observed that microwave measurements at the Ka band were sensitive to plant stress. They found a correlation between a polarization index based on vertical and horizontal microwave measurements at the Ka band and a measured crop water stress index over corn. A coefficient of correlation of 0.92 was obtained for measurements performed with an incidence angle of 50°. Other authors treated the vegetation canopy more or less as an "interference factor" that hinders direct estimation of the soil moisture from microwave emission (Jackson and Schmugge, 1991; Joseph et al., 2010; Wigneron et al., 1993, 2004, among others).

Diurnal Dynamics of Backscattering in Crop Canopies

Since the late 1970s, various studies reported diurnal variations in the backscattering coefficient of crop canopies. This was attributed to variations in the dielectric properties of the canopy caused by changes in the vegetation moisture status (Brisco et al., 1990; Ulaby and Batlivala, 1976) and to changes in the geometrical properties related to leaf orientation (Brisco et al., 1990).

A diurnal pattern in backscattering in a wheat canopy was observed by Brisco et al. (1990) using a truck-mounted L-, C-, and Ku-band scatterometer. However, these patterns were dependent on the frequencies investigated. The difference in patterns was explained by an increased geometric effect in the backscattering at higher frequency. The diurnal changes in backscattering were also dependent on the status of the crop. In the vegetative stage (June), diurnal changes were mostly controlled by the vegetation water content, whereas at the senescing stage (July, August), diurnal backscattering changes were controlled by soil backscattering. They also observed that cross-polarization measurements (VH, HV) resulted in smaller diurnal changes of the backscattering than the copolarized channels (HH, VV), especially for C- and L-band frequencies. Forster et al. (1991) observed that the diurnal changes in X-band radar backscattering from water-stressed tomato canopy plants were dependent on frequency and incidence angles. Brakke et al. (1981) measured diurnal backscattering from ground-based microwave radar at the Ku band (13 GHz), VV polarization, and 50° incidence angle for wheat, corn, and sorghum. Surprisingly, they did not found any correlation between the backscattering and either leaf water potential or wind speed. However, their data set was relatively limited.

Seasonal Dynamics of Backscattering in Crop Canopies

Seasonal variations in the backscattering coefficient in crop canopies were also investigated by several authors. The backscattering coefficients of sugarbeet (*Beta vulgaris* L.) and potato were determined by Bouman and Van Kasteren (1990a) using X-band radar over a period of 6 yr. They observed a saturation level in backscattering coefficients when crops reached a soil cover of 80%. Changes in the geometry of a crop–soil system caused by strong winds, thinning of plants, as well as architecture of individual plants were found to affect backscattering. The authors concluded that radar backscattering across the various years was highly variable due to interplay of different environmental factors influencing canopy geometry. Paris (1986) presented results of combined backscattering and biophysical parameters obtained during the growing season of corn. He found a clear power law relationship between the backscattering cross section of a corn leaf and its LAI. Peak values of canopy LAI coincided with measured backscattering coefficients observed at a 50° incidence angle both in HH and VV polarization. The time of the onset of the reproductive process in the corn plant was clearly detected in the temporal evolution of the backscattering coefficient. The surface soil moisture effect on the backscattering coefficient was insignificant at the Ku band (17 GHz), except at the end of the season when the corn was nearly transparent to the radiation.

Characterization of Crop Canopies Using Air- and Spaceborne Remote Sensing

Active Systems

Table 3 also provides an overview of remotely sensed backscattering using aircraft and satellite platforms for agricultural crops. Most of these studies were conducted in the framework of large measurement campaigns operated at regional scale. A major difference with the experiments conducted using ground-based equipment is the fact that the obtained backscattering is typically related to averaged ground-based measurements of soils and vegetation obtained at different fields. Often the timing of ground-truth sampling shows a time lag with respect to the overpasses. This might not be a problem for quantities that differ only slightly in time lag such as LAI, biomass, and plant height. Evidence from diurnal measurements, however, shows that this might be different for vegetation water content and canopy structure. The latter may be strongly affected by stress effects and wind conditions and may lead to additional noise on measured signals which cannot be related to a specific process. Ferrazzoli (2002) concluded on the basis of a literature review that correlations between backscattering and vegetation parameters obtained from airborne campaigns were not as good as the ones obtained from multitemporal single-field ground-based observations.

A main motivation for using radar remote sensing is crop classification (Bouman and Van Kasteren, 1990a), which is primarily based on the characterization of crop geometry. Hereby, differences in phenological development of, for example, wheat, barley (*Hordeum vulgare* L.), and oat (*Avena sativa* L.) may lead to different temporal signatures in the backscattering. Skriver et al. (1999) found that the correlation between HH and VV polarization backscattering from C- and L-band SAR was suitable for discriminating between winter and spring crops, especially for the C band. Discrimination at early stages between both types of crops may help in further distinguishing individual crops belonging to one of these categories based on the temporal evolution of such correlations. Recently, Skriver et al. (2011) used short-revisit multitemporal C- and L-band SAR data for crop classification. They found that multitemporal acquisitions are very important for single- and dual-polarization modes and that cross-polarized backscattering provided the best results.

Airborne and spaceborne radars have also been used to better understand the influence of vegetation on the signal backscattering. Brown et al. (1992) used airborne SAR data of different frequencies (L, C, and X bands) to measure backscattering from different canopies and found that correlation between C- and L-band and between X- and L-band data were very low, indicating that the radar backscattering at the different frequencies was caused by different mechanisms. Especially for vertical oriented crops such as wheat, a low correlation was found for the X and C bands, whereas

the correlation was found to be acceptable for broad-leaved plants such as canola (*Brassica napus* L.) and field pea (*Pisum sativum* L.). Additionally, the backscattering determined at the L band was found to be more sensitive to the soil moisture content.

Several studies investigated the potential use of spaceborne radar for agricultural purposes, such as crop type mapping, crop condition assessment, soil tillage, crop residue mapping, soil moisture estimation, and monitoring crop growth (McNairn and Brisco, 2004). In the past, spaceborne SAR sensors (e.g., ERS-1, ERS-2, JERS-1, RADARSAT-1) were limited to a single frequency and polarization. To obtain enough information for agriculture applications, multichannel radar observations were required. Recently several improvements were made to increase the information content in the SAR data sets, such as the addition of polarizations (ASAR/ENVISAT, RADARSAT-2), the use of additional frequencies (TerraSAR-X, COSMO-SkyMed, and PALSAR/ALOS), and the integration of SAR data with other frequencies and optical sensors that can provide additional crop and soils information (Clevers and vanLeeuwen, 1996; McNairn and Brisco, 2004). Nevertheless, information on the sensitivity of SAR measurements to crop condition indicators is still limited (McNairn and Brisco, 2004). Wigneron et al. (2002) found limitations in the retrieval of vegetation biomass of sunflower using ERS-2/SAR C-band data. This was attributed to the long revisit period (35 d), which was deemed not sufficient for monitoring of the sunflower vegetation cycle. In addition, accuracy of retrievals of the parametric growth curve was low. Recently, Baghdadi et al. (2009) examined the potential of three SAR sensors (TerraSAR-X, ASAR/ENVISAT, PALSAR/ALOS) operating at different frequencies (X, C, and L bands) for mapping the harvest of sugarcane. The authors showed a high correlation between backscattering coefficient and Normalized Difference Vegetation Index (NDVI) independently estimated from SPOT-4/5 images over the same fields. The best discrimination between plowed and vegetated sugarcane (*Saccharum officinarum* L.) fields was obtained by TerraSAR-X data. They also showed that cross-polarization channels have more potential than copolarization channels for the detection of the sugarcane harvest.

A correct assessment of vegetation water content is essential for the accurate prediction of backscattering and emission from crop canopies as well as for the exact assessment of surface soil moisture content. In addition, vegetation water content could be an important indicator for the presence of water stress in crop canopies, as well as the phenological stage of the canopy. Taconet et al. (1994) found a negative correlation between X-band backscattering and vegetation water content in wheat from airborne radar with no dependency on the soil moisture content. Additionally, accuracies in estimated crop water content were the same at 20 and 40° incidence angle and higher for HH polarization than for VV polarization. A saturation effect of the radar cross section was observed as the canopy becomes denser. Saatchi et al. (1994) developed an algorithm to retrieve canopy water content of natural grassland and pastures from airborne SAR data. Le Vine and Karam (1996) analyzed the dependence of attenuation in a vegetation canopy on frequency and plant water content in a synthetic study to examine the hypothesis that attenuation in vegetation is proportional to the water content of the canopy. Therefore, they used the concept of optical depth (τ) with $\tau = b \times \mathrm{VWC}$ (see Eq. [5]). The results indicated that the hypothesis is not unreasonable for canopies whose structure are small (e.g., leaves, stalks, stems, branches) compared to wavelength. This study was performed to find an appropriate correction of the measured signal for the vegetation canopy to retrieve soil moisture information instead of using the information for canopy characterization.

Passive Systems

In the past, most of the studies performed with airborne or spaceborne radiometers were focused on the retrieval of soil moisture. The vegetation was systematically considered as an attenuation factor in the soil moisture retrieval (Njoku et al., 2000; Wigneron et al., 2004). Recently, several authors used spaceborne radiometer data to characterize the vegetation mostly based on vegetation indices that were derived from the data. These vegetation indices include Microwave Polarization Difference Temperatures (MPDT) (Choudhury and Tucker, 1987), Microwave Polarization Difference Index (MPDI) (Becker and Choudhury, 1988; Kirdyashev et al., 1979), and Microwave Vegetation Indices (MVIs) (Shi et al., 2008). Shi et al. (2008) developed a set of MVIs based on data from AMSR-E. The microwave vegetation indices were defined as the intercept (a) and slope (b) derived from a linear relationship between the brightness temperatures observed at two adjacent radiometer frequencies. The MVIs were correlated to the NDVI derived from Moderate Resolution Imaging Spectroradiometer onboard ENVISAT (MODIS) data. They found that the MVIs can provide additional information on crop status since the microwave measurements were sensitive not only to the leafy part of the vegetation but also to the properties of the overall vegetation canopy. Similarly, Chen et al. (2009) found a new MVI for SMOS through the analysis of simulations by the advanced integral equation model. The polarization difference for the bare surface emission signals at different view angles can be well characterized by a linear function with parameters that are dependent on the pair of view angles to be used. This makes it possible to minimize the surface emission signal and maximize the vegetation signal when using multiangular SMOS measurements. Zhao et al. (2011) found that the MVIs are a function of vegetation water content or vegetation transmissivity. The b parameter of MVIs decreased with increased vegetation water content but increased with increased vegetation transmissivity. Finally, the authors used the MVIs for the correction of vegetation effects in soil moisture retrieval over areas with sparse vegetation in the Tibet Plateau. Li et al. (2010) analyzed the relationship between MPDT, MPDI, and MVIs for the case of cotton (*Gossypium hirsutum* L.). They showed that MPDT and MPDI were negatively correlated to vegetation water

content. For the specific case of cotton, they showed that MVIs are more suitable to retrieve vegetation water content. Jones et al. (2011) used passive microwave information from AMSR-E (Ku band) to quantify global patterns and seasonal variability in vegetation optical depth (VOD) over a 6-yr record (2003–2008). The VOD parameter showed significant correlation with vegetation indices and LAI obtained from MODIS optical-infrared data and phenology cycles over 82% of the global domain. It has to be noted that dual-polarized and multiangular L-band data from SMOS have also the ability to gain information on both soil moisture content and VOD.

Canopy Dielectric and Plant Water Properties

Vegetation Dielectric Properties

As already stated, backscattering and emission retrieved by active and passive systems are directly affected by the dielectric properties of the soil–plant system and might therefore be used for early water stress detection in crop stands because the amount of water in the crop canopy is generally the dominant factor controlling the dielectric properties (Nelson, 1991). Unfortunately, the dielectric properties also depend on measurement frequency, canopy and soil temperature, density and structure of the vegetation (Nelson, 1991), and the salinity of the plant water (Ulaby and Jedlicka, 1984). Therefore, the relationship between dielectric permittivity and canopy water content is not straightforward. Among the first who systematically analyzed the dependency of dielectric permittivity and canopy water content were Ulaby and Jedlicka (1984), who treated the wet vegetation as a two-component mixture of bulk water (including air) and water. On the basis of these assumptions they developed two phase mixing models where the dielectric permittivity of the vegetation mixture (namely the stalk material), water, and bulk vegetation was assumed to differ in total amounts (and therefore differ in total influence on the overall signal). Unfortunately, none of the developed two-phase mixing models could describe measured data at the X band (8 GHz). As a consequence they increased the complexity of the models by using a three-component random-needle mixing model, where the bulk vegetation was used as a host material and the air and water as randomly orientated needle-like inclusions. This approach already agreed well with measured data at the X band (8 GHz). Finally, they proposed a four-phase refractive mixing model consisting of the bulk vegetation as a host, and three additional types of inclusion, such as (i) air, (ii) free water with a fixed dielectric permittivity for the frequency range used, and (iii) bound water with an ice-like dielectric permittivity. Applying this complex model the measured data were fitted as good as with the simpler three-phase mixing model. Therefore, the authors concluded that the problem of modeling the dielectric properties of water contained in a given material was not well understood at the time. On the basis of this work, Ulaby and El-Rayes (1987) developed a Debye–Cole dual-dispersion dielectric model consisting of a component that accounts for the volume fraction occupied by water in free form and another that accounts for the volume fraction occupied by the mixture comprised of water molecules bound to bulk-vegetation molecules. The model was again tested against measured data and showed excellent agreement over a wide range of moisture conditions and within the frequency range 0.2 to 20 GHz. Additionally, Ulaby and El-Rayes (1987) found that the bound water content increases with decreasing total water content. A number of authors developed mixing models for specific purposes or vegetation compartments, such as the dielectric model for leaves as proposed by Mätzler (1994), and for various plants, such as Shrestha et al. (2005, 2007).

Diurnal Changes in Plant Water and Dielectric Properties

Within the biological and agronomy community it is widely known that diurnal changes of plant water content might occur as a consequence of water stress induced by high temperatures and/or shortening of available soil moisture. Ackley (1954) observed diurnal and seasonal changes in crop water content and water deficit of crops. He clearly demonstrated that leaf water content drops to its minimum in the early afternoon and recovered during night time. In the following years various studies indicated that not only the water content but also the turgor pressure change during the day (Acevedo et al., 1979; Ackerson et al., 1977; Allen et al., 1998; Dutt and Gill, 1978; Ehrler et al., 1978; Olsson and Milthorpe, 1983; Turner, 1974, among many others), whereby the changes were highly dependent on the crop type (Turner, 1974). From a plant physiological point of view it is also clear that the turgor pressure is much more sensitive to stress conditions than the total plant water content. This has been proven by studies from Dutt and Gill (1978), for example, who showed that even small changes in water content correspond to relatively large changes in turgor pressure. Additionally, Ehrler et al. (1978), Forster et al. (1991), and Olsson and Milthorpe (1983) showed the existence of a diurnal hysteretic effect in the leaf water potential as a function of the induced water stress in the soil. Hereby, the recovery of plant water potential tended to be slower for plants that are undergoing water stress compared to nonstressed plants.

Backscattering coefficients were also found to be sensitive to changes in leaf water potential, as reported by Forster et al. (1991), Martin et al. (1989), and Siddique et al. (2000). However, further research is needed to explore dependencies between canopy properties such as leaf water potential, leaf water content, and canopy geometry and radar backscattering. To complement the information from plant observations these dependencies need to be related to the observed water status in soil using soil moisture content and soil matric potential measurements. In addition, the value of combined passive and active microwave measurements in characterizing the dynamics of canopy geometry needs to be explored. There is evidence in literature that changes in canopy geometry may strongly contribute to the observed backscattering (see below). In addition, geometric effects appear to be more

important in backscattering from active microwave systems than in signals obtained by passive systems.

Factors Controlling Microwave Signals of Crop Canopies

In this section, we will discuss the various factors that may lead to changes in the structure and function of crop canopies, and that, therefore, may affect the observed microwave emission and backscattered signals. Some of these factors have already been addressed in previous sections and will only be briefly mentioned. The presentation below shows that many environmental factors may influence the observed microwave signals and that disentangling their influence needs both monitoring of these factors but also quantification of their effect on microwave signals. The identification of water stress phenomena in particular may be confounded by other effects also inducing changes in canopy structure and function. Also, environmental controls, such as soil moisture status and microclimatology, may affect microwave signals. Identification of water stress may therefore require monitoring of all relevant parameters and properties affecting microwave emission and backscattering.

Water Stress Phenomena

The relation between water stress and microwave emissions and backscattering was already partly addressed. In this subsection we will mainly focus on the effect of water stress on crop canopy structure and function. It is well known from crop physiology that water or drought stress in plants may lead to changes in the structure and function of the canopy and thereby affect the observed microwave emission or backscattering coefficient. Depending on the intensity and severity of this stress, the effects may range from fully reversible to irreversible. Despite this effect of plant water status on microwave emission of its canopy due to changes in its structural properties, there are practically no studies available in the literature that allow relating water stress, the related changes in geometrical properties of the canopy, and, for example, backscattering coefficients or microwave emission. Water stress effects that may be detected by microwave techniques include: (i) loss of turgor pressure in the leaves leading to the droop of leaves (Singh et al., 2006), (ii) reduced cell division and thus reduced stem elongation leading to changes in LAI and plant height (Song et al., 2008), (iii) changes in leaf structure to reduce transpiration losses (Moran et al., 1989), and (iv) reduced capability in tracking sunlight (Moran et al., 1989). Most of these effects, however, have typically been studied with optical and near-infrared sensors (Colwell, 1974; Moran et al., 1989). Droop of ears in spring barley was observed by Cookmartin et al. (2000) using microwave methods. This droop of ears led to a substantial increase in their radar cross section. Most likely this effect was caused by stress conditions, but no clear evidence was given by the authors. The study by Colpitts and Coleman (1997) analyzed drought stress of a potato leaf using measurements in the L, C, and Ku bands. Drought stress could be related directly to reduced leaf gravimetric water content and leaf thickness. They found only weak statistical relationships between complex relative permittivity and the gravimetric moisture content of a leaf because the water/air ratio within the leaf remained nearly constant with changing water content. In contrast, correlations were found between leaf permittivity and leaf thickness across the wavelengths used. The leaf thickness was found to be directly related to relative leaf water content, osmotic potential, water potential, and turgor pressure. These findings suggest that the canopy architecture will have a much stronger effect on radar backscattering than the permittivity.

Wind Strength

It appears that the effect of wind strength on radar backscattering is important for measurements performed at high frequencies. These findings and the importance for retrieving canopy water stress from backscattering measurements of wind strength, however, need to be further validated. In early publications, such as Brakke et al. (1981), no effect of wind speed on the radar backscattering measured at the Ku band and two different polarizations was found for corn, sorghum, and wheat. Wu et al. (1985b) observed strong fading of the backscattering signal in milo due to wind effects using the X band. Bouman and Van Kasteren (1990a) used the X band to analyze factors that influence backscattering coefficient of potato and sugarbeet and found that the architecture of individual beet plants and their distribution in space affected the radar backscattering. Strong winds especially led to changes in canopy architecture and therefore will affect radar backscattering and may confound the quantification of water stress phenomenon.

Saturation Effect

The quantification of saturation effect is mainly an issue for active systems, especially at higher frequencies. Saturation implies that the backscattering coefficient becomes insensitive to changes in canopy structure and function (Blaes et al., 2006; Cookmartin et al., 2000; Liu et al., 2006; Taconet et al., 1994). Occurrence of saturation effects have been related to the type of crop (Bouman and Van Kasteren, 1990a; Ferrazzoli et al., 1997), crop biomass (Bouman and Van Kasteren, 1990a), crop cover (Bouman, 1991), crop height (McNairn et al., 2000), and LAI (Blaes et al., 2006; Ferrazzoli et al., 1992) and may mask potential correlation between crop parameters and backscattering coefficient (Chen et al., 2009). In addition, saturation has been observed at different polarizations and incidence angles (Chen et al., 2009; Ferrazzoli et al., 1992; McNairn and Brisco, 2004).

Only a few studies analyzed the effect of vegetation water content on the occurrence of saturation. Taconet et al. (1994) used the airborne scatterometer ERASME in the C and X bands, HH and VV polarization, and incidence angles 15 to 45°. Backscattering coefficients were obtained for 2 yr under different soil moisture conditions for wheat. Backscattering values obtained with the X band using HH polarization saturated at vegetation water contents

larger than 3 kg m^{-2} and became highly variable for values larger than 4 kg m^{-2}. A similar pattern was observed for values observed in the X band using VV polarization. Bouman (1991) used radar backscattering data at the X band to derive crop parameter from beet, potato, barley, and wheat. In the case of beet, the backscattering coefficients obtained saturation values at a fraction cover of 0.8, with values ranging between 0 and −2 dB. Backscattering coefficients for potato were found to saturate at a similar fraction cover but with values ranging between −2 and −4 dB. For wheat and barley no saturation level could be observed. For beet, crop water content at the fraction cover of 0.8 was about 0.5 kg m^{-2}, whereby between 0.8 and full cover the crop water content increased up to 6 kg m^{-2} and more, indicating that radar backscattering no longer corresponded to changes in vegetation water content (their Fig. 1 and 7a). Therefore, the presence of saturation effect may mask the detection of water stress in plant canopies. Saturation effects may also be observed for microwave signals obtained from radiometers. Wigneron et al. (1993) used a multifrequency radiometer (PORTOS) to monitor the microwave emission of a soybean field. Both soil moisture and biomass parameterized by the vegetation volume fraction were found to have a very significant effect on the evolution of the microwave signal. Increase in biomass led to saturation of the observed emissions at 5.05 and 36.5 GHz, but this effect was less pronounced at 1.4 GHz, showing a continuous increase of the microwave signal.

Surface Soil Moisture Content

Surface soil moisture content is a key variable in understanding mass and energy transfer processes between the land surface and the atmosphere, whereby passive and active microwave systems have extensively been used to determine its spatial and temporal dynamics. However, exact estimation of soil moisture content from emission or backscattering is hampered by the presence of a vegetation canopy. To overcome the problem of the confounding signal from the vegetation canopy, radiative transfer models were developed and applied which account for all processes within the vegetation canopy (Hunt et al., 2011; Joseph et al., 2010). The derivation of crop parameters from microwave methods may be hampered by the influence of the underlying soil, and more specifically, by changes in the soil moisture content, especially for frequencies lower than the C band. In this respect, vegetation canopy models may be extremely valuable to derive properties that can provide information on the status of the canopy, and its water status in particular.

Several findings have shown that the soil surface moisture status determines the intensity of the observed radar backscattering of cropped soil. For example, Ulaby et al. (1982) found that at 50% of field capacity the backscattering of a radar operating at 4.25 to 4.75 GHz (10° incidence angle) was dominated by the vegetation. Additionally, radar backscattering seemed to be dominated by the return from the soil at higher moisture contents. Airborne scatterometer (X band with HH polarization) data of wheat fields showed no clear dependence of the backscattering signal on soil moisture content (Taconet et al., 1994). Additionally, a negative correlation between radar backscattering and vegetation water content was found for the frequency used. They found that at lower frequencies (C band) and steep to medium incidence angles, the radar backscattering comes from the underlying soil attenuated through the vegetation above. Similarly, Baghdadi et al. (2009) showed that for L-band measurements performed at 20° incidence angle over a fully grown sugarcane crop (50 cm high) the radar signal was no longer sensitive to surface roughness and the sensitivity to soil moisture content was low (around 0.04 dB [%, v/v]). Detecting crop emergence may be masked by dips and peaks in the backscattering caused by changes in soil moisture content (Bouman and Van Kasteren, 1990a). Joseph et al. (2008) used the ratio between modeled bare soil backscattering and the vegetation water content to estimate surface soil moisture using dual-polarized L-band measurements (1.6 GHz). The authors also reported that the retrieval of soil moisture was found to be dependent on the view angle and polarization used, whereby they found best agreement at 35° view angle and VV polarization. Encouraged by the positive results Joseph et al. (2010) used also successfully C-band data to estimate soil moisture content. Contradictory to these findings Schoups et al. (1998) reported that for the S and even C bands, the radar signal becomes less sensitive to soil moisture content and surface roughness and more sensitive to canopy parameters.

Also, the characterization of vegetation canopy using passive microwave measurements is affected by the surface soil moisture status. Hornbuckle and England (2004), for example, reported that there was still a radiometric sensitivity in the L band to soil moisture even under corn having a biomass of 8.0 kg m^{-2}. One way to exclude the effect of soil moisture on the total emission and radar backscattering was the installation of a perfect reflector above the ground. Brunfeldt and Ulaby (1984) analyzed the effect of vegetation on microwave emission and radar backscattering in a systematical sense by applying this technique. Therefore, the soil between the crop rows was covered by a perfect reflector to block emissions from the soil and reflect downwelling radiation from the vegetation. Additionally, uncovered reference fields were used to validate their simplified radiative transfer model. Overall, the model performed well, but the authors also clearly indicated that more research is needed to understand emission and reflection from crop stands. Calvet et al. (2011) analyzed the sensitivity of passive microwave observations to soil moisture content and vegetation water content for frequencies ranging between the L and W bands. They showed that for frequencies higher than the L band a larger sensitivity was observed to vegetation water content than to surface soil moisture content.

Biophysical Crop Parameter

Microwave methods have extensively been used to characterize biophysical crop parameters. Most of this work has been done by relating backscattering coefficients from active microwave

methods to observed crop parameters under field conditions. In the subsequent discussion, we will briefly present some major findings regarding key parameters such as crop biomass, LAI, and plant geometry. Biomass and LAI will be discussed together since most microwave studies typically provide information on both quantities (Table 3). Other properties, such as plant height, crop cover, and growing stage, will be referred to as we present these key parameters.

Crop Biomass and Leaf Area Index

Many studies have shown that there is a clear interdependence between biomass, LAI and observed backscattering coefficients from active microwave systems. A large number of these studies are listed in Table 3, and they provide regression equations and coefficient of correlation to express the performance of the derived relationships. Rather than presenting these relationships in detail we would like to highlight some issues that are of importance when conducting microwave experiments to derive such dependencies. Analysis of these studies showed that canopy properties other than biomass and LAI may confound the expected relationship between both properties and the observed backscattering. These properties included the growing stage of the crop (Bouman and Hoekman, 1993; Bouman and Van Kasteren, 1990a) and the canopy structure and geometry (Bouman and Hoekman, 1993; Bouman and Van Kasteren, 1990a), but also the soil moisture status (Brakke et al., 1981; Brown et al., 1992; Martin et al., 1989; Mattia et al., 2003), environmental conditions (Hoekman and Bouman, 1993), and management properties (Paris, 1983). It is therefore mandatory to monitor these confounding factors when trying to relate biomass and LAI to observed backscattering coefficients.

The specific growing stage of the crop has been shown to be an important factor determining the relationship between biomass, LAI, and backscattering. The effect of growth stage was often related to geometry and saturation effects. C-band HH backscattering data from ASAR obtained over winter wheat was found to correlate very well with biomass ($R^2 > 0.65$), LAI and other parameters, such as plant water content, leaf water content per unit leaf area, and specific growing stages, such as regreening (Liu et al., 2006). In the same study backscattering signals from VV polarization were also analyzed but typically showed less correlation than values obtained with HH polarization, independently of the growth stage. During booting and milking stages temporal changes in the correlation were observed with lower correlations both for HH and VV polarization. On the other hand, pooling of regreening and booting data resulted in high correlations between C-band HH backscattering, biomass, and LAI. Negative correlations between biomass and C-band HH and VV backscattering ($R^2 = -0.52$ and -0.44) were found at booting. This was explained by changes in the canopy structure. The low correlations between biomass and also LAI observed from the C-band HH backscattering may be due to saturation. Blaes et al. (2006) showed that VV/HH polarization ratios obtained at incidence angles between 35 and 45° were able to assess the crop growth until saturation of the signal was reached (LAI of 4.6).

Several studies specifically focused on the analysis between LAI and backscattering coefficients. Ulaby and Jedlicka (1984), for example, studied the relationship between LAI and backscattering measured at frequencies ranging between 8.6 and 35.6 GHz over corn, sorghum, and wheat. Most of the observed variation in canopy backscattering could be explained through variations in green LAI for cases where the LAI was greater than 0.5. For the wheat crop, the correlation was only good before head formation started. Again the authors observed an important contribution of the soil backscattering at early growth stages with low LAI (<0.5). The relationship between LAI of rice (*Oryza sativa* L.) and the C-band VV/HH backscattering ratio was analyzed by Chen et al. (2009), who found highest correlation for LAI values ranging between 1.7 and 3.5.

The above discussion of confounding factors showed that the effect of these parameters on backscattering depends also on the type of polarization and the incidence angles used. Singh (2006) performed ground-based X-band measurements at different angles and polarizations to analyze the relationship between biophysical parameters of soybean such as plant height, biomass, LAI, and crop covered soil moisture. He found the highest correlation between biomass and backscattering for incidence angles larger than 40° and VV polarization. Lower angles were more affected by dynamics in soil moisture. Brown et al. (2003) used C- and X-band measurements to estimate the biomass of an outdoor wheat canopy. They showed that a two-channel C band operating at moderate incidence angles was most appropriate to estimate biomass. The authors argued that biomass was expressed through its effect on extinction, rather than by its contribution to backscattering. Differential attenuation of soil backscattering by the HH and VV polarization (i.e., the difference between both polarizations) was found to best relate to biomass. However, the period with a large biomass increase was not captured. Mattia et al. (2003) used ground-based C-band backscattering measurements on wheat fields to derive relationship between wheat biomass and soil moisture. They showed that biomass could not be retrieved using VV polarization with an incidence angle of 23° due to modulation from soil moisture. Better results were obtained for biomass prediction from backscattering when using the VV/HH ratio with an incidence angle of 40°. Maity et al. (2004) assumed a linear relationship between LAI and crop height for analysis with RADARSAT, whereby the increase in LAI and plant height led to an increase in backscattering. All studies analyzed suggest that the derivation of relationships between biomass and backscattering coefficient was most successful for larger incidence angles and that lower frequencies may result in better estimates.

Effects of Leaves, Stems, and Branches

Most of the work on the effects of geometry and related plant parts on microwave signals has been done using active measurements

systems and has focused on specific parts of the plants such as leaves, stems, and branches. Characterizing these elements in terms of electromagnetic properties and shapes is essential for any mathematical modeling of backscattering coefficients. Several studies have shown that the leaf size and leaf geometry greatly influence the observed backscattering coefficients (Brown et al., 2003; Karam and Fung, 1989; Wu et al., 1985b). Paris (1986) was one of the first to include the leaf size in a modified water cloud model to predict backscattering from a corn canopy and obtained an excellent fit between modeled and observed backscattering at a frequency of 17.5 GHz. Paloscia (1998) showed that the change in backscattering with vegetation water content was different for wide-leaf crops (grains) and crops with circular leaves (sunflowers). She concluded that crops with the same vegetation water content may result in different backscattering due to the geometry of the leaves. Cookmartin et al. (2000) showed that nonplanarity of leaves in oilseed rape was a considerable source of error in the physically based radiative transfer model RT2. An additional mechanisms was observed by Della Vecchia et al. (2006), who reported that leaf curvature of maize and stem hollowness of wheat led to a reduction of backscattering and stem attenuation from the C band, respectively. Further analysis showed that these effects seem to be dependent on the growth stage of the crop. In addition to leaf shape and size, stem, ear, and branch properties also influence backscattering of radar signals. To overcome these problems and to allow interpretation of ERS-2 backscattering data, Cookmartin et al. (2000) developed an equivalent integratable first-order radiative transfer model that included a correct representation of attenuation by the stems and scattering by ears in cereals crops.

Management Practices

Finally, management practices also may play an important role in the analysis of backscattering signals. Paris (1983) found that radar backscattering coefficients were affected by row directions among fields cropped with corn, soybean, alfalfa, and wood when using like-polarization at look angles between 5 and 25°. No effects were found for cross-polarization or look angles greater than 25° independent of the polarization. Additionally, wet surface soil water conditions, typical for irrigated crop systems, were less favorable than dry surface conditions for distinguishing between crop types. The effect of row direction of wheat and barley, for example, was smaller than the effect of row spacing. A close row spacing of 12.5 cm for wheat and barley resulted in relatively high backscattering values during early vegetative growth and low backscattering values at grain filling and ripening compared to larger row spacing. This effect of row spacing was only observed at low and medium frequencies. Even the removal or preservation of crop residues and plowing and harrowing of the stubble will influence the backscattering coefficient of X-band measurements, as reported by Bouman and Van Kasteren (1990a).

Multisensors Measurements

For the characterization of crop conditions (i.e., type, status, height), the use of more than one sensor type gives valuable information. Data acquired for the same site by different sensors are partially redundant, since they represent the same location, and partially complementary, since the sensors have different characteristics and the physical mechanisms of diffusion are different (Le Hegarat-Mascle et al., 2000). Several approaches to combine microwave data from several frequencies, active with passive microwave, or microwave data with optical data from visible, near infrared, and thermal spectra have been published. These methods are discussed in the following. We will focus on the combination of active and passive systems and on the combination of microwave with optical/multispectral systems. However, Dong et al. (2009) and Pohl and van Genderen (1998) reviewed the topic and found that real fusion techniques for disparate data that actually contribute to the understanding of the objects observed are rare.

Active and Passive Microwave Sensors

In several early studies, passive and active microwave signatures of various agricultural crops were measured, for example, by Brunfeldt and Ulaby (1984) and Hüppi (1987). At this stage, a strong focus was on the estimation of soil moisture, considering vegetation as a confounding factor only for soil moisture retrieval (Jackson et al., 1982). Saatchi et al. (1994) developed an active/passive microwave scattering model for a grass canopy to explain the behavior of reduction in sensor sensitivity to soil moisture in the presence of a (wet) thatch layer. Chauhan (1997) used NASA's AIRSAR to estimate the vegetation opacity and surface roughness, whereas the brightness temperature was received by the Push-Broom Microwave Radiometer (PBMR). The study was mainly focused on the estimation of soil moisture, but they showed well the synergistic effect of active and passive microwave sensors to gain information about the status of cropped agricultural fields. As a consequence of the upcoming SMAP mission (Njoku et al., 2010), the combined use of active and passive microwave data is gaining more attention, whereby the focus of SMAP lies in the estimation of near surface soil moisture (Dorigo et al., 2010).

An exception from the focus on soil moisture retrieval is the work of Wigneron et al. (1999), who simulated active and passive observations to investigate the surface characteristics over a soybean field. Soil and vegetation effects were best described by combining passive microwave data at the L band with multiangle active microwave data at the C band. Similarly, Jin and Huang (1996) developed a model considering an agricultural crop stand as a layer of continuous random media with an underlying rough surface. They analyzed the correlations of active and passive microwave signatures for different crops and compared them to real measurements at 1.2 GHz. The results showed that simultaneous radar and radiometer observations can be efficiently used to monitor the development of agricultural crops. Moreover, they identified

clusters in emissivity and backscattering, which were used to separate different vegetation types. Oza et al. (2008) used SSM/I (passive) and Quickscat (active) data for the identification of rice growing stages from transplanting to maturity. While SSM/I was better able to identify the transplantation period, Quickscat was better able to predict the heading phase. Unfortunately, a real fusion of active and passive microwave data was not performed. A study using the ground-based radiometer–scatterometer system RASAM (Hüppi, 1987) and a feed forward neural network for biomass estimation of oat and wheat was presented by Jin and Liu (1997). This was also not a real data fusion, but they jointly used active and passive microwave signals for the retrieval of biomass characteristics including canopy height, canopy water content, and dry matter fraction in an adequate accuracy.

Microwave and Optical/Multispectral Sensors

While the microwave scattering process is influenced by the structural elements of the land cover, optical sensors provide either information on the chemical composition (hyperspectral sensors) or physical temperature (IR sensors) of the scene. Therefore, a fusion of these two data sets is feasible, especially for characterization of the plant status (Huang et al., 2010). Important fusion techniques are the principal component analysis (PCA) and the intensity–hue–saturation (IHS) transform. Additive Integration, Component Substitution, and Intensity Modulation are fusion methods tested by Chibani (2006) using SPOT and RADARSAT-1 data. However, most studies just compared the microwave signals to vegetation indices (Baghdadi et al., 2009; Hunt et al., 2011; Jones et al., 2011; Rosenthal et al., 1985; Svoray and Shoshany, 2002).

Real combination or fusion of microwave and optical signals for the characterization of crop canopies are rare, but would provide reasonable information. In general, two categories of microwave and optical data fusion techniques are reported.

The first category includes approaches aiming at an enhanced land cover and land use discrimination. Hereby, methods such as IHS transform and PCA transfer the remote sensing data into a new system, which introduces severe radiometric distortions, or they even lose their physical meaning, but enhance the spatial separability of land cover classes. Wavelet-based methods (Amolins et al., 2007)—even the simplest—tend to produce better results than standard fusion schemes such as IHS and PCA. Typically, wavelet fusion schemes have been proposed to import detailed information from SAR into multispectral imagery. The advantage is that the multispectral information remains almost unchanged and the texture information from SAR will be transferred. For classification approaches, a significant change in the data characteristics can be accepted because a classification traditionally makes use of the relative differences between the classes only. Horgan et al. (1992) as well as Vescovi and Gomarasca (1999) fused shuttle imaging radar and Landsat data for enhanced classification. Similarly, Smara et al. (1998) and Michelson et al. (2000) found higher class separabilities when Landsat TM and ERS-1 data were combined. Alparone et al. (2004) presented a similar study on the succession satellites Landsat ETM+ and ERS-2 data with a wavelet transform. Le Hegarat-Mascle et al. (2000) fused multitemporal ERS images and multispectral Landsat images by the Dempster-Shafer evidence theory for unsupervised classification to use their complementarity in reducing confusion by getting more complete description of the land cover type features. Haack and Khatiwada (2010) applied a spectral signature extraction and Transformed Divergence approach for SIR-C and Landsat data. Hong et al. (2009) developed a combined IHS-Wavelet Fusion algorithm. Finally, McNairn et al. (2009) analyzed the performance of different classification algorithms on fused data sets of Radarsat-1, ASAR, SPOT, and Landsat.

The second category includes approaches that aim at a more detailed identification of absolute crop conditions. A combined use of optical and radar remote sensing was presented by Dente et al. (2008), who assimilated LAI derived from MERIS and ASAR into a crop growth model for yield estimation. It has to be mentioned that the combination of microwave and optical data was only used for gap filling of time series within the study. Mangiarotti et al. (2008) used a bi-objective optimization method to assimilate ASAR backscattering and SPOT-Vegetation NDVI into a vegetation dynamics model to improve its predictions on biomass and LAI, whereas Hadria et al. (2010) performed a comparative analysis using time series of both FORMOSAT-2 and ASAR images for the monitoring of irrigated wheat crops in a semiarid region in Morocco. Hereby, FORMOSAT-2 images were used to characterize the spatiotemporal variations of green LAI, which was incorporated into a simple canopy functioning model to provide spatial estimates of above-surface biomass and topsoil moisture. They found evidence that the signal reaches a saturation level from intermediate values of biomass water content ($\sim$2000 g m^{-2}). Airborne Visible and Infrared Imaging Spectrometer (AVIRIS) and AirSAR data were fused by Huang et al. (2010) for the estimation of fractions of nonphotosynthetic vegetation (grass and shrub). This approach may also give feasible information on the conditions of dried crops, such as cereals before harvest.

In general, the utilization of multisensor and multifrequency information leads to a better characterization of the crop status. The approaches mentioned may be feasible to identify plant stress related differences to the normal crop growth. However, for this goal more work is needed on the development of new sensors and fusion algorithms in an applicable way.

Outlook

We reviewed the use of microwave methods to characterize crop canopies using microwave methods and with specific focus on their ability to identify the presence of water stress related phenomena.

Our analysis of the literature showed that practically no data sets are available that provide both microwave measurements of the plant canopy (e.g., backscattering, optical depth) and detailed measurements of the physiological properties of the canopy, the soil moisture status, and the microclimatic conditions in the canopy, and therefore, allow evaluating observed microwave signals in relation to stress phenomena. Measurements presented in the literature and related to analyzing the effect of water stress on, for example, microwave signals were typically conducted on single plants under lab conditions with little information on the soil and plant water status. Moreover, there are no data available that provide information on soil and plant water status in combination with microwave measurements at the field scale. Detailed temporal and spatially distributed information about the soil and plant water status is in our opinion essential when evaluating any remote sensing method used to assess the occurrence and presence of water stress in plants. Microwave measurements should therefore be combined with measurements of soil water potential and soil moisture content in the root zone, micrometeorological measurements within and above the canopy as well as physiological properties and quantities of the plant such as volume–pressure curves, vegetation water content, leaf water potential, and transpiration rate of the plant. The characterization of geometrical and structural properties of the canopy and their dynamical behavior is another essential element to assess the effect of water stress phenomena on microwave signals. Interpretation of such integrated data sets in combination with three-dimensional functional, structural plant canopy models including the effects of physiological processes on the radiative transfer properties of the canopy will improve early identification of stress and will help to disentangle the factors influencing observed microwave signals. It will help to better evaluate the importance of mapping the dynamics and spatial distribution of surface soil moisture in terms of identifying the occurrence of plant water stress at the field scale. Up to now it is not clear in how far information on surface soil moisture status is relevant in assessing early plant water stress.

A combination of different sensor technologies covering the full spectral range from optical to microwave will open new perspectives and generate new knowledge about the status of vegetation and more specifically crop canopies. A first attempt to combine this spectral range on one platform that was suitable for crop science applications was ESA's ENVISAT mission, launched in 2002. For future satellites there is a trend to develop specialized sensors on individual platforms, such as the five planned ESA Sentinels (1: C-Band SAR, 2: Superspectral, 3: Ocean, 4/5: Atmospheric Chemistry) will continue the work of actual missions. Moreover, German activities around TerraSAR-X, TanDEM-X, RapidEye, EnMAP, and Tandem-L provides and will provide sound knowledge about plant conditions and will in combination be able to identify crop stress. Myneni and Choudhury (1993) already pointed at the potential of combining different sensor technologies. They stated that combining optical and microwave techniques will allow observing different responses of the plants due to water stress, such as the diurnal response of water stress detectable by microwave methods, but which does not occur in the pigment concentration. Moreover, a combination of optical and microwave data can be synergistically used to infer land surface properties and crop status. Also, optical data and their deduced parameters can be used for correction and interpretation of microwave observations.

Here a close cooperation between the soil, plant, and remote sensing communities may lead to new results. In addition, validation of these novel model approaches will require data that are presently not available in literature as already outlined above.

Assimilation of remotely sensed properties, such as backscattering coefficient or brightness temperature, may provide a unique opportunity to improve the estimate of biophysical properties as crop canopies, such as LAI, dry matter, plant water content, and related leaf potential, and others. Initial studies that use assimilation of remotely sensed microwave data have been developed recently in the field of hydrology (Draper et al., 2011; Montzka et al., 2011), meteorology (Rasmy et al., 2011), or for optical remote sensed data and the assimilation in crop functioning models (Weiss et al., 2001). However, this avenue has not been really pursued in the past for vegetation canopy properties for microwave frequencies, but it provides a huge potential for remotely sensed data, especially for microwave data, as they are available for almost all weather conditions. Within the field of microwave measurements, acquisition of backscattering data at different frequency bands may provide additional information on the status of the crop. Lopez-Sanchez and Ballester-Berman (2009) stated that a combination of low and high microwave bands allows determination of different properties of the plants and different scales of their components, such as leaves, stems, and heads. Additionally, multipolarization (dual and full polarization) data exploit the sensitivity of the wave polarization to the orientation, shape, and dielectric properties of the elements in the scene. Therefore, polarimetry SAR interferometry (such as PolInSAR) seems to be the most promising tool to gain information for agricultural crop stands (Lopez-Sanchez and Ballester-Berman, 2009). Finally, PolInSAR yields information not only about the dielectric properties, shape, and orientation of the whole plant constituents, but also about the vertical structure of the plant by means of information about the localization of the scattering centers.

Appendix

AirSAR: NASA's Airborne Synthetic Aperture Radar
AMSR-E: Advanced Microwave Scanning Radiometer onboard the Earth Observing System
ALOS: Advanced Land Observing Satellite
AQUARIUS: NASA's sea surface salinity mission
ASAR: Advanced Synthetic Aperture Radar onboard ENVISAT

ASCAT: MetOp's Advanced SCATterometer, the successor to the C-Band scatterometers flown on ESA's ERS-1 and ERS-2 satellites
AVIRIS: Airborne Visible and Infrared Imaging Spectrometer
COSMO-SkyMed: Constellation of small Satellites for Mediterranean basin Observation
EnMAP: German hyperspectral Environmental Mapping and Analysis Program
ERS-1 & 2: European Remote Sensing Satellite 1 and 2
ENVISAT: ESA's Environmental Satellite
ETM+: Landsat Enhanced Thematic Mapper Plus (Landsat 7)
FORMOSAT-2: Taiwan Earth imaging satellite 2
JERS-1: Japanese Earth Resources Satellite 1
Landsat TM: Landsat Thematic Mapper (Landsat 5)
MAPS: Multifrequency polarimetric scatterometer
MERIS: Medium Resolution Imaging Spectrometer onboard ENVISAT
MIRAS: Microwave Imaging Radiometer with Aperture Synthesis onboard SMOS
MODIS: Moderate Resolution Imaging Spectroradiometer onboard ENVISAT
PALSAR: Phased Array type L-band Synthetic Aperture Radar onboard ALOS
PBMR: Push-Broom Microwave Radiometer
PolInSAR: Polarimetric interferometric SAR
PORTOS: Six-frequency radiometer of the Institut National de Recherches Agronomiques (INRA) Avignon, France.
Radarsat-1 & 2: Canadian Space Agency's radar satellite 1 & 2
RapidEye: System of 5 multi-spectral satellites
RASAM: Radiometer-Scatterometer to Measure Microwave Signatures of Soil, Vegetation and Snow
SAC-D: Satélite de Aplicaciones Científicas, platform of AQUARIUS
SAR: Synthetic Aperture Radar
SMAP: NASA's Soil Moisture Active Passive Mission
SIR-A: Shuttle Imaging Radar A L-Band Synthetic Aperture Radar flown 1981 on Space Shuttle
SIR-C/X SAR: Spaceborne Imaging Radar-C/X-Band Synthetic Aperture Radar flown 1994 on Space Shuttle
SMOS: ESA's Soil Moisture and Ocean Salinity Mission
SPOT: Satellite Pour l'Observation de la Terre (Satellite for Earth Observation)
SSM/I: Special Sensor Microwave Imager
Quickscat: NASA's Quick Scatterometer
Tandem-L: Proposed L-Band Radar Mission
TanDEM-X: TerraSAR-X add-on for Digital Elevation Measurement
TerraSAR-X: German X-Band Radar Mission
WindSAT: Multi-channel multi-frequency microwave radiometer for Ocean Surface Wind detection

Acknowledgments
This study was supported by the German Research Foundation DFG (Transregional Collaborative Research Centre 32—Patterns in Soil–Vegetation–Atmosphere Systems: Monitoring, modeling and data assimilation).

References

Acevedo, E., E. Fereres, T.C. Hsiao, and D.W. Henderson. 1979. Diurnal growth trends, water potential, and osmotic adjustment of maize and sorghum leaves in the field. Plant Physiol. 64(3):476–480. doi:10.1104/pp.64.3.476

Ackerson, R.C., D.R. Krieg, T.D. Miller, and R.E. Zartman. 1977. Water relations of field-grown cotton and sorghum- temporal and diurnal changes in leaf water, osmotic, and turgor potentials. Crop Sci. 17:76–80. doi:10.2135/cropsci1977.0011183X001700010022x

Ackley, W.B. 1954. Seasonal and diurnal changes in the water contents and water deficits of Bartlett pear leaves. Plant Physiol. 29(5):445–448. doi:10.1104/pp.29.5.445

Allen, L.H., R.R. Valle, J.W. Jones, and P.H. Jones. 1998. Soybean leaf water potential responses to carbon dioxide and drought. Agron. J. 90:375–383. doi:10.2134/agronj1998.00021962009000030010x

Alparone, L., S. Baronti, A. Garzelli, and F. Nencini. 2004. Landsat ETM+ and SAR image fusion based on generalized intensity modulation. IEEE Trans. Geosci. Rem. Sens. 42(12):2832–2839. doi:10.1109/TGRS.2004.838344

Amolins, K., Y. Zhang, and P. Dare. 2007. Wavelet based image fusion techniques—An introduction, review and comparison. ISPRS J. Photogramm. Remote Sens. 62(4):249–263. doi:10.1016/j.isprsjprs.2007.05.009

Attema, E.P.W., and F.T. Ulaby. 1978. Vegetation modeled as a water cloud. Radio Sci. 13(2):357–364. doi:10.1029/RS013i002p00357

Baghdadi, N., N. Boyer, P. Todoroff, M. El Hajj, and A. Begue. 2009. Potential of SAR sensors TerraSAR-X, ASAR/ENVISAT and PALSAR/ALOS for monitoring sugarcane crops on Reunion Island. Remote Sens. Environ. 113(8):1724–1738. doi:10.1016/j.rse.2009.04.005

Battaglia, A., M.O. Ajewole, and C. Simmer. 2006. Evaluation of radar multiple-scattering effects from a GPM perspective. Part I: Model description and validation. J. Appl. Meteorol. Climatol. 45(12):1634–1647. doi:10.1175/JAM2424.1

Becker, F., and B.J. Choudhury. 1988. Relative sensitivity of normalized difference vegetation index (NDVI) and microwave polarization difference index (MPDI) for vegetation and desertification monitoring. Remote Sens. Environ. 24:297–311. doi:10.1016/0034-4257(88)90031-4

Blaes, X., and P. Defourny. 2003. Retrieving crop parameters based on tandem ERS 1/2 interferometric coherence images. Remote Sens. Environ. 88:374–385. doi:10.1016/j.rse.2003.08.008

Blaes, X., P. Defourny, U. Wegmüller, A. Della Vecchia, L. Guerriero, and P. Ferrazzoli. 2006. C-band polarimetric indexes for maize monitoring based on a validated radiative transfer model. IEEE Trans. Geosci. Rem. Sens. 44(4):791–800. doi:10.1109/TGRS.2005.860969

Bouman, B.A.M. 1991. Crop parameter-estimation from ground-based X-band (3-cm wave) radar backscattering data. Remote Sens. Environ. 37:193–205. doi:10.1016/0034-4257(91)90081-G

Bouman, B.A.M., and D.H. Hoekman. 1993. Multitemporal, multifrequency radar measurements of agricultural crops during the Agriscatt-88 campaign in the Netherlands. Int. J. Remote Sens. 14(8):1595–1614. doi:10.1080/01431169308953988

Bouman, B.A.M., D.W.G. van Kraalingen, W. Stol, and H.J.C. van Leeuwen. 1999. An agroecological modeling approach to explain ERS SAR radar backscatter of agricultural crops. Remote Sens. Environ. 67:137–146. doi:10.1016/S0034-4257(98)00079-0

Bouman, B.A.M., and H.W.J. van Kasteren. 1990a. Ground-based X-band (3-cm wave) radar backscattering of agricultural crops. 1. Sugar-beet and potato—Backscattering and crop growth. Remote Sens. Environ. 34:93–105. doi:10.1016/0034-4257(90)90101-Q

Bouman, B.A.M., and H.W.J. van Kasteren. 1990b. Ground-based X-band (3-cm wave) radar backscattering of agricultural crops. 2. Wheat, barley, and oats—The impact of canopy structure. Remote Sens. Environ. 34:107–119. doi:10.1016/0034-4257(90)90102-R

Bracaglia, M., P. Ferrazzoli, and L. Guerriero. 1995. A fully polarimetric multiple scattering model for crops. Remote Sens. Environ. 54:170–179. doi:10.1016/0034-4257(95)00151-4

Brakke, T.W., E.T. Kanemasu, J.L. Steiner, F.T. Ulaby, and E. Wilson. 1981. Microwave radar response to canopy moisture, leaf-area index, and dry-weight of wheat, corn, and sorghum. Remote Sens. Environ. 11:207–220. doi:10.1016/0034-4257(81)90020-1

Brisco, B., R.J. Brown, J.A. Koehler, G.J. Sofko, and M.J. Mckibben. 1990. The diurnal pattern of microwave backscattering by wheat. Remote Sens. Environ. 34:37–47. doi:10.1016/0034-4257(90)90082-W

Brown, R.J., M.J. Manore, and S. Poirier. 1992. Correlations between X-band, C-band, and L-band imagery within an agricultural environment. Int. J. Remote Sens. 13(9):1645–1661. doi:10.1080/01431169208904218

Brown, S.C.M., S. Quegan, K. Morrison, J.C. Bennett, and G. Cookmartin. 2003. High-resolution measurements of scattering in wheat canopies- Implications for crop parameter retrieval. IEEE Trans. Geosci. Rem. Sens. 41:1602–1610. doi:10.1109/TGRS.2003.814132

Brunfeldt, D.R., and F.T. Ulaby. 1984. Measured microwave emission and scattering in vegetation canopies. IEEE Trans. Geosci. Rem. Sens. 22:520–524.

Bush, T.F., and F.T. Ulaby. 1976. Radar return from a continuous vegetation canopy. IEEE Trans. Antenn. Propag. 24(3):269–276. doi:10.1109/TAP.1976.1141352

Calvet, J.C., J.P. Wigneron, J. Walker, F. Karbou, A. Chanzy, and C. Albergel. 2011. Sensitivity of passive microwave observations to soil moisture and vegetation water content: L-band to W-band. IEEE Trans. Geosci. Rem. Sens. 49:1190–1199. doi:10.1109/TGRS.2010.2050488

Chauhan, N.S. 1997. Soil moisture estimation under a vegetation cover: Combined active passive microwave remote sensing approach. Int. J. Remote Sens. 18:1079–1097. doi:10.1080/014311697218584

Chen, J.S., H. Lin, C.D. Huang, and C.Y. Fang. 2009. The relationship between the leaf area index (LAI) of rice and the C-band SAR vertical/horizontal (VV/HH) polarization ratio. Int. J. Remote Sens. 30(8):2149–2154. doi:10.1080/01431160802609700

Chibani, Y. 2006. Additive integration of SAR features into multispectral SPOT images by means of the a trous wavelet decomposition. ISPRS J. Photogramm. Remote Sens. 60(5):306–314. doi:10.1016/j.isprsjprs.2006.05.001

Choudhury, B.J., and C.J. Tucker. 1987. Monitoring global vegetation using Nimbus-7 37 Ghz Data—Some empirical relations. Int. J. Remote Sens. 8:1085–1090. doi:10.1080/01431168708954754

Chukhlantsev, A.A., A.M. Shutko, and S.P. Golovachev. 2003. Attenuation of electromagnetic waves by vegetation canopies. J. Commun. Technol. Electron. 48:1177–1202.

Clevers, J.G.P.W., and H.J.C. vanLeeuwen. 1996. Combined use of optical and microwave remote sensing data for crop growth monitoring. Remote Sens. Environ. 56:42–51. doi:10.1016/0034-4257(95)00227-8

Colpitts, B.G., and W.K. Coleman. 1997. Complex permittivity of the potato leaf during imposed drought stress. IEEE Trans. Geosci. Rem. Sens. 35:1059–1064. doi:10.1109/36.602547

Colwell, J.E. 1974. Vegetation canopy reflectance. Remote Sens. Environ. 3:175–183. doi:10.1016/0034-4257(74)90003-0

Cookmartin, G., P. Saich, S. Quegan, R. Cordey, P. Burgess-Allen, and A. Sowter. 2000. Modeling microwave interactions with crops and comparison with ERS-2 SAR observations. IEEE Trans. Geosci. Rem. Sens. 38:658–670. doi:10.1109/36.841996

Del Frate, F., P. Ferrazzoli, L. Guerriero, T. Strozzi, U. Wegmüller, G. Cookmartin, and S. Quegan. 2004. Wheat cycle monitoring using radar data and a neural network trained by a model. IEEE Trans. Geosci. Rem. Sens. 42:35–44. doi:10.1109/TGRS.2003.817200

Della Vecchia, A., P. Ferrazzoli, and L. Guerriero. 2004. Modelling microwave scattering from long curved leaves. Waves Random Media 14(2):S333–S343. doi:10.1088/0959-7174/14/2/012

Della Vecchia, A., P. Ferrazzoli, L. Guerriero, L. Ninivaggi, T. Strozzi, and U. Wegmüller. 2008. Observing and modeling multifrequency scattering of maize during the whole growth cycle. IEEE Trans. Geosci. Rem. Sens. 46:3709–3718. doi:10.1109/TGRS.2008.2001885

Della Vecchia, A., P. Ferrazzoli, J.P. Wigneron, and J.P. Grant. 2007. Modeling forest emissivity at L-band and a comparison with multitemporal measurements. IEEE Geosci. Remote Sens. Lett. 4(4):508–512. doi:10.1109/LGRS.2007.900687

Della Vecchia, A., K. Saleh, P. Ferrazzoli, L. Guerriero, and J.P. Wigneron. 2006. Simulating L-band emission of coniferous forests using a discrete model and a detailed geometrical representation. IEEE Geosci. Remote Sens. Lett. 3(3):364–368. doi:10.1109/LGRS.2006.873230

Dente, L., G. Satalino, F. Mattia, and M. Rinaldi. 2008. Assimilation of leaf area index derived from ASAR and MERIS data into CERES-Wheat model to map wheat yield. Remote Sens. Environ. 112:1395–1407. doi:10.1016/j.rse.2007.05.023

Detar, W.R., J.V. Penner, and H.A. Funk. 2006. Airborne remote sensing to detect plant water stress in full canopy cotton. Trans. ASABE 49(3):655–665.

Dong, J., D.F. Zhuang, Y.H. Huang, and J.Y. Fu. 2009. Advances in multi-sensor data fusion: Algorithms and applications. Sensors (Basel Switzerland) 9(10):7771–7784. doi:10.3390/s91007771

Dorigo, W.A., K. Scipal, R.M. Parinussa, Y.Y. Liu, W. Wagner, R.A.M. de Jeu, and V. Naeimi. 2010. Error characterisation of global active and passive microwave soil moisture datasets. Hydrol. Earth Syst. Sci. 14(12):2605–2616. doi:10.5194/hess-14-2605-2010

Draper, C., J.F. Mahfouf, J.C. Calvet, E. Martin, and W. Wagner. 2011. Assimilation of ASCAT near- surface soil moisture into the SIM hydrological model over France. Hydrol. Earth Syst. Sci. 15(12):3829–3841. doi:10.5194/hess-15-3829-2011

Dutt, S.K., and K.S. Gill. 1978. Diurnal changes in leaf water potential of rice, barley and wheat. Biol. Plant. 20(6):472–474. doi:10.1007/BF02923354

Ehrler, W.L., S.B. Idso, R.D. Jackson, and R.J. Reginato. 1978. Diurnal changes in plant water potential and canopy temperature of wheat as affected by drought. Agron. J. 70:999–1004. doi:10.2134/agronj1978.00021962007000060027x

Eom, H.J., and A.K. Fung. 1984. A scatter model for vegetation up to Ku-band. Remote Sens. Environ. 15(3):185–200. doi:10.1016/0034-4257(84)90030-0

Ferrazzoli, P. 2002. SAR for agriculture: Advances, problems and prospects. Proceedings of the Third International Symposium on Retrieval of Bio- and Geophysical Parameters from SAR Data for Land Applications. ESA Special Publications. ESA Publications Division.

Ferrazzoli, P., and L. Guerriero. 1996. Passive microwave remote sensing of forests: A model investigation. IEEE Trans. Geosci. Rem. Sens. 34:433–443. doi:10.1109/36.485121

Ferrazzoli, P., S. Paloscia, P. Pampaloni, G. Schiavon, S. Sigismondi, and D. Solimini. 1997. The potential of multifrequency polarimetric SAR in assessing agricultural and arboreous biomass. IEEE Trans. Geosci. Rem. Sens. 35(1):5–17. doi:10.1109/36.551929

Ferrazzoli, P., S. Paloscia, P. Pampaloni, G. Schiavon, D. Solimini, and P. Coppo. 1992. Sensitivity of Microwave Measurements to Vegetation Biomass and Soil-Moisture Content- a Case-Study. IEEE Trans. Geosci. Rem. Sens. 30(4):750–756. doi:10.1109/36.158869

Forster, R.R., C.E. Martin, and R.K. Moore. 1991. Radar backscatter correlation with leaf water potential of water-stressed tomato canopies. In: IEEE Geoscience and Remote Sensing Symposium, 1991. IGARSS '91, p. 2269–2272.

Fung, A.K. 1994. Microwave scattering and emission models and their application. Artech House, Boston, MA.

Gomez-Dans, J.L., S. Quegan, and J.C. Bennett. 2006. Indoor C-band polarimetric interferometry observations of a mature wheat canopy. IEEE Trans. Geosci. Rem. Sens. 44(4):768–777. doi:10.1109/TGRS.2005.863861

Govender, M., P.J. Dye, I.M. Weiersbye, E.T.F. Witkowski, and F. Ahmed. 2009. Review of commonly used remote sensing and ground-based technologies to measure plant water stress. Water S.A. 35(5):741–752. doi:10.4314/wsa.v35i5.49201

Guglielmetti, M., M. Schwank, C. Matzler, C. Oberdorster, J. Vanderborght, and H. Fluhler. 2007. Measured microwave radiative transfer properties of a deciduous forest canopy. Remote Sens. Environ. 109(4):523–532. doi:10.1016/j.rse.2007.02.003

Guglielmetti, M., M. Schwank, C. Matzler, C. Oberdorster, J. Vanderborght, and H. Fluhler. 2008. FOSMEX: Forest soil moisture experiments with microwave radiometry. IEEE Trans. Geosci. Rem. Sens. 46(3):727–735. doi:10.1109/TGRS.2007.914797

Haack, B.N., and G. Khatiwada. 2010. Comparison and integration of optical and quadpolarization radar imagery for land cover/use delineation. J. Appl. Remote Sens. 4:043507. doi:10.1117/1.3328873

Hadria, R., B. Duchemin, L. Jarlan, G. Dedieu, F. Baup, S. Khabba, A. Olioso, and T. Le Toan. 2010. Potentiality of optical and radar satellite data at high spatio-temporal resolutions for the monitoring of irrigated wheat crops in Morocco. Int. J. Appl. Earth Obs. Geoinf. 12:S32–S37. doi:10.1016/j.jag.2009.09.003

Hoekman, D.H., and B.A.M. Bouman. 1993. Interpretation of C-band and X-band radar images over an agricultural area, the Flevoland test site in the Agriscatt-87 campaign. Int. J. Remote Sens. 14(8):1577–1594. doi:10.1080/01431169308953987

Hong, G., Y. Zhang, and B. Mercer. 2009. A wavelet and IHS integration method to fuse high resolution SAR with moderate resolution multispectral images. Photogramm. Eng. Remote Sens. 75(10):1213–1223.

Hong, S., and I. Shin. 2011. A physically-based inversion algorithm for retrieving soil moisture in passive microwave remote sensing. J. Hydrol. 405(1–2):24–30. doi:10.1016/j.jhydrol.2011.05.005

Horgan, G.W., C.A. Glasbey, S.L. Soria, J.N.C. Gozalo, and F.G. Alonso. 1992. Land-use classification in central Spain using Sir-a and Mss imagery. Int. J. Remote Sens. 13(15):2839–2848. doi:10.1080/01431169208904085

Hornbuckle, B.K., and A.W. England. 2004. Radiometric sensitivity to soil moisture at 1.4 GHz through a corn crop at maximum biomass. Water Resour. Res. 40(10):W10204. doi:10.1029/2003WR002931

Hornbuckle, B.K., A.W. England, R.D. De Roo, M.A. Fischman, and D.L. Boprie. 2003. Vegetation canopy anisotropy at 1.4 GHz. IEEE Trans. Geosci. Rem. Sens. 41(10):2211–2223. doi:10.1109/TGRS.2003.817192

Huang, S.L., C. Potter, R.L. Crabtree, S. Hager, and P. Gross. 2010. Fusing optical and radar data to estimate sagebrush, herbaceous, and bare ground cover in Yellowstone. Remote Sens. Environ. 114(2):251–264. doi:10.1016/j.rse.2009.09.013

Hunt, E.R., L. Li, M.T. Yilmaz, and T.J. Jackson. 2011. Comparison of vegetation water contents derived from shortwave-infrared and passive-microwave sensors over central Iowa. Remote Sens. Environ. 115(9):2376–2383. doi:10.1016/j.rse.2011.04.037

Hüppi, R.A. 1987. RASAM: A radiometer-scatterometer to measure microwave signatures of soil, vegetation and snow. University of Bern, Bern.

Jackson, T.J. 1993. Measuring surface soil-moisture using passive microwave. 3. Remote sensing. Hydrol. Processes 7(2):139–152. doi:10.1002/hyp.3360070205

Jackson, T.J., and P.E. O'Neill. 1990. Attenuation of soil microwave emission by corn and soybeans at 1.4 Ghz and 5 Ghz. IEEE Trans. Geosci. Rem. Sens. 28(5):978–980. doi:10.1109/36.58989

Jackson, T.J., and T.J. Schmugge. 1989. Passive microwave remote-sensing system for soil-moisture- some supporting research. IEEE Trans. Geosci. Rem. Sens. 27(2):225–235. doi:10.1109/36.20301

Jackson, T.J., and T.J. Schmugge. 1991. Vegetation effects on the microwave emission of soils. Remote Sens. Environ. 36(3):203–212. doi:10.1016/0034-4257(91)90057-D

Jackson, T.J., T.J. Schmugge, and J.R. Wang. 1982. Passive microwave sensing of soil-moisture under vegetation canopies. Water Resour. Res. 18(4):1137–1142. doi:10.1029/WR018i004p01137

Jin, Y.Q., and X.Z. Huang. 1996. Correlation of temporal variations of active and passive microwave signatures from vegetation canopy. IEEE Trans. Geosci. Rem. Sens. 34(1):257–263. doi:10.1109/36.481910

Jin, Y.Q., and C. Liu. 1997. Biomass retrieval from high-dimensional active/passive remote sensing data by using artificial neural networks. Int. J. Remote Sens. 18(4):971–979. doi:10.1080/014311697218863

Jonard, F., L. Weihermüller, K.Z. Jadoon, M. Schwank, H. Vereecken, and S. Lambot. 2011. Mapping field-scale soil moisture with L-band radiometer and ground-penetrating radar over bare soil. IEEE Trans. Geosci. Rem. Sens. 49(8):2863–2875. doi:10.1109/TGRS.2011.2114890

Jones, M.O., L.A. Jones, J.S. Kimball, and K.C. McDonald. 2011. Satellite passive microwave remote sensing for monitoring global land surface phenology. Remote Sens. Environ. 115(4):1102–1114. doi:10.1016/j.rse.2010.12.015

Joseph, A.T., R. van der Velde, P.E. O'Neill, R. Lang, and T. Gish. 2010. Effects of corn on C- and L-band radar backscatter: A correction method for soil moisture retrieval. Remote Sens. Environ. 114(11):2417–2430. doi:10.1016/j.rse.2010.05.017

Joseph, A.T., R. van der Velde, P.E. O'Neill, R.H. Lang, and T. Gish. 2008. Soil moisture retrieval during a corn growth cycle using L-band (1.6 GHz) radar observations. IEEE Trans. Geosci. Rem. Sens. 46(8):2365–2374. doi:10.1109/TGRS.2008.917214

Karam, M.A., and A.K. Fung. 1989. Leaf-shape effects in electromagnetic-wave scattering from vegetation. IEEE Trans. Geosci. Rem. Sens. 27(6):687–697. doi:10.1109/TGRS.1989.1398241

Kirdyashev, K.P., A.A. Chukhlantsev, and A.M. Shutko. 1979. Microwave radiation of grounds with vegetative cover. Radiotekhnika I Elektronika 24(2):256–264.

Le Hegarat-Mascle, S., A. Quesney, D. Vidal-Madjar, O. Taconet, M. Normand, and C. Loumagne. 2000. Land cover discrimination from multitemporal ERS images and multispectral Landsat images: A study case in an agricultural area in France. Int. J. Remote Sens. 21(3):435–456. doi:10.1080/014311600210678

Le Vine, D.M., and M.A. Karam. 1996. Dependence of attenuation in a vegetation canopy on frequency and plant water content. IEEE Trans. Geosci. Rem. Sens. 34(5):1090–1096. doi:10.1109/36.536525

Li, Y.Q., L.X. Zhang, L.M. Jiang, Z.J. Zhang, and T.J. Zhao. 2010. Evaluation of vegetation indices based on microwave data by simulation and measurements. In: IEEE International Symposium on Geoscience and Remote Sensing IGARSS, p. 3311–3314.

Liu, L.Y., J.J. Wang, Y.S. Bao, W.J. Huang, Z.H. Ma, and C.J. Zhao. 2006. Predicting winter wheat condition, grain yield and protein content using multi-temporal EnviSat-ASAR and Landsat TM satellite images. Int. J. Remote Sens. 27(4):737–753. doi:10.1080/01431160500296867

Liu, S.F., Y.A. Liou, W.J. Wang, J.P. Wigneron, and J.B. Lee. 2002. Retrieval of crop biomass and soil moisture from measured 1.4 and 10.65 GHz brightness temperatures. IEEE Trans. Geosci. Rem. Sens. 40(6):1260–1268. doi:10.1109/TGRS.2002.800277

Lopez-Sanchez, J.M., and J.D. Ballester-Berman. 2009. Potentials of polarimetric SAR interferometry for agriculture monitoring. Radio Sci. 44:RS2010. doi:10.1029/2008RS004078

Lu, D.S. 2006. The potential and challenge of remote sensing-based biomass estimation. Int. J. Remote Sens. 27(7):1297–1328. doi:10.1080/01431160500486732

Macelloni, G., S. Paloscia, P. Pampaloni, and R. Ruisi. 2001. Airborne multifrequency L- to Ka-band radiometric measurements over forests. IEEE Trans. Geosci. Rem. Sens. 39(11):2507–2513. doi:10.1109/36.964988

Maity, S., C. Patnaik, M. Chakraborty, and S. Panigrahy. 2004. Analysis of temporal backscattering of cotton crops using a semiempirical model. IEEE Trans. Geosci. Rem. Sens. 42(3):577–587. doi:10.1109/TGRS.2003.821888

Mangiarotti, S., P. Mazzega, L. Jarlan, E. Mougin, F. Baup, and J. Demarty. 2008. Evolutionary bi-objective optimization of a semi-arid vegetation dynamics model with NDVI and sigma(0) satellite data. Remote Sens. Environ. 112(4):1365–1380. doi:10.1016/j.rse.2007.03.030

Marliani, F., S. Paloscia, P. Pampaloni, and J.A. Kong. 2002. Simulating coherent backscattering from crops during the growing cycle. IEEE Trans. Geosci. Rem. Sens. 40(1):162–177. doi:10.1109/36.981358

Martin, R.D., G. Asrar, and E.T. Kanemasu. 1989. C-band scatterometer measurements of a tallgrass prairie. Remote Sens. Environ. 29(3):281–292. doi:10.1016/0034-4257(89)90007-2

Mattia, F., T. Le Toan, G. Picard, F.I. Posa, A. D'Alessio, C. Notarnicola, A.M. Gatti, M. Rinaldi, G. Satalino, and G. Pasquariello. 2003. Multitemporal C-band radar measurements on wheat fields. IEEE Trans. Geosci. Rem. Sens. 41(7):1551–1560. doi:10.1109/TGRS.2003.813531

Mätzler, C. 1990. Seasonal evolution of microwave-radiation from an oat field. Remote Sens. Environ. 31(3):161–173. doi:10.1016/0034-4257(90)90086-2

Mätzler, C. 1994. Microwave (1–100 Ghz) dielectric model of leaves. IEEE Trans. Geosci. Rem. Sens. 32(4):947–949. doi:10.1109/36.298024

McNairn, H., and B. Brisco. 2004. The application of C-band polarimetric SAR for agriculture: A review. Can. J. Rem. Sens. 30(3):525–542. doi:10.5589/m03-069

McNairn, H., C. Champagne, J. Shang, D. Holmstrom, and G. Reichert. 2009. Integration of optical and Synthetic Aperture Radar (SAR) imagery for delivering operational annual crop inventories. ISPRS J. Photogramm. Remote Sens. 64(5):434–449. doi:10.1016/j.isprsjprs.2008.07.006

McNairn, H., J.J. van der Sanden, R.J. Brown, and J. Ellis. 2000. The potential of RADARSAT-2 for crop mapping and assessing crop condition. In: Second International Conference on Geospatial Information in Agriculture and Forestry, Lake Buena Vista, FL.

Michelson, D.B., B.M. Liljeberg, and P. Pilesjo. 2000. Comparison of algorithms for classifying Swedish landcover using Landsat TM and ERS-1 SAR data. Remote Sens. Environ. 71(1):1–15. doi:10.1016/S0034-4257(99)00024-3

Montzka, C., H. Moradkhani, L. Weihermüller, H.-J. Hendricks Franssen, M. Canty, and H. Vereecken. 2011. Hydraulic parameter estimation by remotely-sensed top soil moisture observations with the particle filter. J. Hydrol. 399:410–421. doi:10.1016/j.jhydrol.2011.01.020

Moran, M.S., P.J. Pinter, B.E. Clothier, and S.G. Allen. 1989. Effect of water-stress on the canopy architecture and spectral indexes of irrigated alfalfa. Remote Sens. Environ. 29(3):251–261. doi:10.1016/0034-4257(89)90004-7

Moran, M.S., A. Vidal, D. Troufleau, J. Qi, T.R. Clarke, P.J. Pinter, T.A. Mitchell, Y. Inoue, and C.M.U. Neale. 1997. Combining multifrequency microwave and optical data for crop management. Remote Sens. Environ. 61(1):96–109. doi:10.1016/S0034-4257(96)00243-X

Myneni, R.B., and B.J. Choudhury. 1993. Synergistic use of optical and microwave data in agrometeorological applications. Adv. Space Res. 13(5):239–248. doi:10.1016/0273-1177(93)90551-L

Nelson, S.O. 1991. Dielectric-properties of agricultural products—Measurements and applications. IEEE Trans. Electr. Insul. 26(5):845–869. doi:10.1109/14.99097

Njoku, E.G., and D. Entekhabi. 1996. Passive microwave remote sensing of soil moisture. J. Hydrol. 184(1–2):101–129. doi:10.1016/0022-1694(95)02970-2

Njoku, E.G., P.E. O'Neill, K.H. Kellogg, W.T. Crow, W.N. Edelstein, J.K. Entin, S.D. Goodman, T.J. Jackson, J. Johnson, J. Kimball, J.R. Piepmeier, R.D. Koster, N. Martin, K.C. McDonald, M. Moghaddam, S. Moran, R. Reichle, J.C. Shi, M.W. Spencer, S.W. Thurman, L. Tsang, and J. Van Zyl. 2010. The soil moisture active passive (SMAP) mission. Proc. IEEE 98(5):704–716. doi:10.1109/JPROC.2010.2043918

Njoku, E.G., W.J. Wilson, S.H. Yueh, and Y. Rahmat-Samii. 2000. A large-antenna microwave radiometer-scatterometer concept for ocean salinity and soil moisture sensing. IEEE Trans. Geosci. Rem. Sens. 38:2645–2655. doi:10.1109/36.885211

Olsson, K.A., and F.L. Milthorpe. 1983. Diurnal and spatial variation in leaf water potential and leaf conductance of irrigated peach-trees. Aust. J. Plant Physiol. 10(3):291–298. doi:10.1071/PP9830291

O'Neill, P.E., N.S. Chauhan, and T.J. Jackson. 1996. Use of active and passive microwave remote sensing for soil moisture estimation through corn. Int. J. Remote Sens. 17(10):1851–1865. doi:10.1080/01431169608948743

Oza, S.R., S. Panigrally, and J.S. Parihar. 2008. Concurrent use of active and passive microwave remote sensing data for monitoring of rice crop. Int. J. Appl. Earth Obs. Geoinf. 10(3):296–304. doi:10.1016/j.jag.2007.12.002

Paloscia, S. 1998. An empirical approach to estimating leaf area index from multifrequency SAR data. Int. J. Remote Sens. 19(2):359–364. doi:10.1080/014311698216323

Paloscia, S., and P. Pampaloni. 1984. Microwave remote-sensing of plant water-stress. Remote Sens. Environ. 16(3):249–255. doi:10.1016/0034-4257(84)90068-3

Paloscia, S., and P. Pampaloni. 1988. Microwave polarization index for monitoring vegetation growth. IEEE Trans. Geosci. Rem. Sens. 26(5):617–621. doi:10.1109/36.7687

Paris, J.F. 1983. Radar backscattering properties of corn and soybeans at frequencies of 1.6, 4.75, and 13.3 Ghz. IEEE Trans. Geosci. Rem. Sens. GE-21(3):392–400. doi:10.1109/TGRS.1983.350472

Paris, J.F. 1986. The effect of leaf size on the microwave backscattering by corn. Remote Sens. Environ. 19(1):81–95. doi:10.1016/0034-4257(86)90042-8

Pellarin, T., J.P. Wigneron, J.C. Calvet, M. Berger, H. Douville, P. Ferrazzoli, Y.H. Kerr, E. Lopez-Baeza, J. Pulliainen, L.P. Simmonds, and P. Waldteufel. 2003. Two-year global simulation of L-band brightness temperatures over land. IEEE Trans. Geosci. Rem. Sens. 41(9):2135–2139. doi:10.1109/TGRS.2003.815417

Picard, G., T. Le Toan, and F. Mattia. 2003. Understanding C-band radar backscatter from wheat canopy using a multiple-scattering coherent model. IEEE Trans. Geosci. Rem. Sens. 41(7):1583–1591. doi:10.1109/TGRS.2003.813353

Pinter, P.J., J.L. Hatfield, J.S. Schepers, E.M. Barnes, M.S. Moran, C.S.T. Daughtry, and D.R. Upchurch. 2003. Remote sensing for crop management. Photogramm. Eng. Remote Sensing 69(6):647–664.

Pohl, C., and J.L. van Genderen. 1998. Multisensor image fusion in remote sensing: Concepts, methods and applications. Int. J. Remote Sens. 19(5):823–854. doi:10.1080/014311698215748

Prasad, R. 2009. Retrieval of crop variables with field-based X-band microwave remote sensing of ladyfinger. Adv. Space Res. 43(9):1356–1363. doi:10.1016/j.asr.2008.12.017

Prévot, L., M. Dechambre, O. Taconet, D. Vidalmadjar, M. Normand, and S. Galle. 1993. Estimating the characteristics of vegetation canopies with airborne radar measurements. Int. J. Remote Sens. 14(15):2803–2818. doi:10.1080/01431169308904310

Rasmy, M., T. Koike, S. Boussetta, H. Lu, and X. Li. 2011. Development of satellite land data assimilation system coupled with mesoscale model in the Tibetan plateau. IEEE Trans. Geosci. Rem. Sens. 49(8):2847–2863. doi:10.1109/TGRS.2011.2112667

Rosenthal, W.D., B.J. Blanchard, and A.J. Blanchard. 1985. Visible infrared microwave agriculture classification, biomass, and plant height algorithms. IEEE Trans. Geosci. Rem. Sens. GE-23(2):84–90. doi:10.1109/TGRS.1985.289404

Saatchi, S.S., D.M. Le Vine, and R.H. Lang. 1994. Microwave backscattering and emission model for grass canopies. IEEE Trans. Geosci. Rem. Sens. 32(1):177–186. doi:10.1109/36.285200

Saleh, K., J.P. Wigneron, P. Waldteufel, P. de Rosnay, M. Schwank, J.C. Calvet, and Y.H. Kerr. 2007. Estimates of surface soil moisture under grass covers using L-band radiometry. Remote Sens. Environ. 109(1):42–53. doi:10.1016/j.rse.2006.12.002

Schmugge, T., P. Gloersen, T. Wilheit, and F. Geiger. 1974. Remote-sensing of soil-moisture with microwave radiometers. J. Geophys. Res. 79(2):317–323. doi:10.1029/JB079i002p00317

Schneeberger, K., M. Schwank, C. Stamm, P. de Rosnay, C. Mätzler, and H. Flühler. 2004. Topsoil structure influencing soil water retrieval by microwave radiometry. Vadose Zone J. 3:1169–1179.

Schoups, G., P.A. Troch, and N. Verhoest. 1998. Soil moisture influences on the radar backscattering of sugar beet fields. Remote Sens. Environ. 65(2):184–194. doi:10.1016/S0034-4257(98)00026-1

Schwank, M., C. Matzler, M. Guglielmetti, and H. Fluhler. 2005. L-band radiometer measurements of soil water under growing clover grass. IEEE Trans. Geosci. Rem. Sens. 43(10):2225–2237. doi:10.1109/TGRS.2005.855135

Serbin, G., and D. Or. 2005. Ground-penetrating radar measurement of crop and surface water content dynamics. Remote Sens. Environ. 96(1):119–134. doi:10.1016/j.rse.2005.01.018

Shi, J.C., T. Jackson, J. Tao, J. Du, R. Bindlish, L. Lu, and K.S. Chen. 2008. Microwave vegetation indices for short vegetation covers from satellite passive microwave sensor AMSR-E. Remote Sens. Environ. 112(12):4285–4300. doi:10.1016/j.rse.2008.07.015

Shrestha, B.L., H.C. Wood, and S. Sokhansanj. 2005. Prediction of moisture content of alfalfa using density-independent functions of microwave dielectric properties. Meas. Sci. Technol. 16(5):1179–1185. doi:10.1088/0957-0233/16/5/018

Shrestha, B.L., H.C. Wood, and S. Sokhansanj. 2007. Modeling of vegetation permittivity at microwave frequencies. IEEE Trans. Geosci. Rem. Sens. 45(2):342–348. doi:10.1109/TGRS.2006.886175

Siddique, M.R.B., A. Hamid, and M.S. Islam. 2000. Drought stress effects on water relations of wheat. Bot. Bull. Acad. Sin. 41(1):35–39.

Singh, D. 2006. Scatterometer performance with polarization discrimination ratio approach to retrieve crop soybean parameter at X-band. Int. J. Remote Sens. 27(19):4101–4115. doi:10.1080/01431160600735988

Singh, D., Y. Yamaguchi, H. Yamada, and K.P. Singh. 2003. Retrieval of wheat chlorophyll by an X-band scatterometer. Int. J. Remote Sens. 24(23):4939–4951. doi:10.1080/0143006031000095961

Singh, V., C.K. Pallaghy, and D. Singh. 2006. Phosphorus nutrition and tolerance of cotton to water stress. I. Seed cotton yield and leaf morphology. Field Crop Sci. 96:191–198. doi:10.1016/j.fcr.2005.06.009

Skriver, H., F. Mattia, G. Satalino, A. Balenzano, V.R.N. Pauwels, N.E.C. Verhoest, and M. Davidson. 2011. Crop classification using short-revisit multitemporal SAR data. IEEE J. Select. Topics Appl. Earth Observ. Remote Sens. 4(2):423–431. doi:10.1109/JSTARS.2011.2106198

Skriver, H., M.T. Svendsen, and A.G. Thomsen. 1999. Multitemporal C- and L-band polarimetric signatures of crops. IEEE Trans. Geosci. Rem. Sens. 37(5):2413–2429. doi:10.1109/36.789639

Smara, Y., A. Belhadj-Aissa, B. Sansal, J. Lichtenegger, and A. Bouzenoune. 1998. Multisource ERS-1 and optical data for vegetal cover assessment and monitoring in a semi-arid region of Algeria. Int. J. Remote Sens. 19(18):3551–3568. doi:10.1080/014311698213812

Song, Y., C. Birch, and J. Hanan. 2008. Analysis of maize canopy development under water stress and incorporation into the ADEL-Maize model. Funct. Plant Biol. 35:925–935. doi:10.1071/FP08055

Stiles, J.M., and K. Sarabandi. 2000. Electromagnetic scattering from grassland Part I: A fully phase-coherent scattering model. IEEE Trans. Geosci. Rem. Sens. 38(1):339–348. doi:10.1109/36.823929

Svoray, T., and M. Shoshany. 2002. SAR-based estimation of areal aboveground biomass (AAB) of herbaceous vegetation in the semi-arid zone: A modification of the water-cloud model. Int. J. Remote Sens. 23(19):4089–4100. doi:10.1080/01431160110115924

Taconet, O., M. Benallegue, D. Vidalmadjar, L. Prevot, M. Dechambre, and M. Normand. 1994. Estimation of soil and crop parameters for wheat from airborne radar backscattering data in C-bands and X-bands. Remote Sens. Environ. 50(3):287–294. doi:10.1016/0034-4257(94)90078-7

Touré, A., K.P.B. Thomson, G. Edwards, R.J. Brown, and B.G. Brisco. 1994. Adaptation of the mimics backscattering model to the agricultural context—Wheat and canola at L and C bands. IEEE Trans. Geosci. Rem. Sens. 32(1):47–61. doi:10.1109/36.285188

Turner, N.C. 1974. Stomatal behavior and water status of maize, sorghum, and tobacco under field conditions. 2. Low soil-water potential. Plant Physiol. 53(3):360–365. doi:10.1104/pp.53.3.360

Ulaby, F.T., A. Aslam, and M.C. Dobson. 1982. Effects of vegetation cover on the radar sensitivity to soil-moisture. IEEE Trans. Geosci. Rem. Sens. GE-20(4):476–481. doi:10.1109/TGRS.1982.350413

Ulaby, F.T., and P.P. Batlivala. 1976. Diurnal-variations of radar backscatter from a vegetation canopy. IEEE Trans. Antenn. Propag. 24(1):11–17. doi:10.1109/TAP.1976.1141298

Ulaby, F.T., and T.F. Bush. 1976a. Corn growth as monitored by radar. IEEE Trans. Antenn. Propag. 24(6):819–828. doi:10.1109/TAP.1976.1141452

Ulaby, F.T., and T.F. Bush. 1976b. Monitoring wheat growth with radar. Photogramm. Eng. Remote Sensing 42(4):557–568.

Ulaby, F.T., and M.A. El-Rayes. 1987. Microwave dielectric spectrum of vegetation. 2. Dual-dispersion model. IEEE Trans. Geosci. Rem. Sens. GE-25(5):550–557. doi:10.1109/TGRS.1987.289833

Ulaby, F.T., and R.P. Jedlicka. 1984. Microwave dielectric-properties of plant materials. IEEE Trans. Geosci. Rem. Sens. GE-22(4):406–415. doi:10.1109/TGRS.1984.350644

Ulaby, F.T., R.K. Moore, and A.K. Fung. 1986. Microwave remote sensing: Active and passive, from theory to applications. Vol. 3. Artech House, Delham, MA.

Ulaby, F.T., K. Sarabandi, K. Mcdonald, M. Whitt, and M.C. Dobson. 1990. Michigan microwave canopy scattering model. Int. J. Remote Sens. 11(7):1223–1253. doi:10.1080/01431169008955090

Ulaby, F.T., and E.A. Wilson. 1985. Microwave attenuation properties of vegetation canopies. IEEE Trans. Geosci. Rem. Sens. GE-23(5):746–753. doi:10.1109/TGRS.1985.289393

Van de Griend, A.A., and J.P. Wigneron. 2004. The b-factor as a function of frequency and canopy type at h-polarization. IEEE Trans. Geosci. Rem. Sens. 42(4):786–794. doi:10.1109/TGRS.2003.821889

Vescovi, F.D., and M.A. Gomarasca. 1999. Integration of optical and microwave remote sensing data for agricultural land use classification. Environ. Monit. Assess. 58(2):133–149. doi:10.1023/A:1006047906601

Wegmüller, U. 1993. Signature research for crop classification by active and passive microwaves. Int. J. Remote Sens. 14(5):871–883. doi:10.1080/01431169308904383

Weiss, M., D. Troufleau, F. Baret, H. Chauki, L. Prevot, A. Olioso, N. Bruguier, and N. Brisson. 2001. Coupling canopy functioning and radiative transfer models for remote sensing data assimilation. Agric. For. Meteorol. 108(2):113–128. doi:10.1016/S0168-1923(01)00234-9

Wigneron, J.P., J.C. Calvet, T. Pellarin, A.A. Van de Griend, M. Berger, and P. Ferrazzoli. 2003. Retrieving near-surface soil moisture from microwave radiometric observations: Current status and future plans. Remote Sens. Environ. 85(4):489–506. doi:10.1016/S0034-4257(03)00051-8

Wigneron, J.P., A. Chanzy, J.C. Calvet, and W. Bruguier. 1995. A simple algorithm to retrieve soil-moisture and vegetation biomass using passive microwave measurements over crop fields. Remote Sens. Environ. 51(3):331–341. doi:10.1016/0034-4257(94)00081-W

Wigneron, J.P., P. Ferrazzoli, J.C. Calvet, Y. Kerr, and P. Bertuzzi. 1999. A parametric study on passive and active microwave observations over a soybean crop. IEEE Trans. Geosci. Rem. Sens. 37(6):2728–2733. doi:10.1109/36.803421

Wigneron, J.P., M. Fouilhoux, L. Prevot, A. Chanzy, A. Olioso, N. Baghdadi, and C. King. 2002. Monitoring sunflower crop development from C-band radar observations. Agronomie 22(6):587–595. doi:10.1051/agro:2002047

Wigneron, J.P., Y. Kerr, A. Chanzy, and Y.Q. Jin. 1993. Inversion of surface parameters from passive microwave measurements over a soybean field. Remote Sens. Environ. 46(1):61–72. doi:10.1016/0034-4257(93)90032-S

Wigneron, J.P., Y. Kerr, P. Waldteufel, K. Saleh, M.J. Escorihuela, P. Richaume, P. Ferrazzoli, P. de Rosnay, R. Gurney, J.C. Calvet, J.P. Grant, M. Guglielmetti, B. Hornbuckle, C. Matzler, T. Pellarin, and M. Schwank. 2007. L-band Microwave Emission of the Biosphere (L-MEB) Model: Description and calibration against experimental data sets over crop fields. Remote Sens. Environ. 107(4):639–655. doi:10.1016/j.rse.2006.10.014

Wigneron, J.P., L. Laguerre, and Y.H. Kerr. 2001. A simple parameterization of the L-band microwave emission from rough agricultural soils. IEEE Trans. Geosci. Rem. Sens. 39(8):1697–1707. doi:10.1109/36.942548

Wigneron, J.P., M. Parde, P. Waldteufel, A. Chanzy, Y. Kerr, S. Schmidl, and N. Skou. 2004. Characterizing the dependence of vegetation model parameters on crop structure, incidence angle, and polarization at L-band. IEEE Trans. Geosci. Rem. Sens. 42(2):416–425. doi:10.1109/TGRS.2003.817976

Wu, L.K., R.K. Moore, and R. Zoughi. 1985a. Sources of scattering from vegetation canopies at 10 Ghz. IEEE Trans. Geosci. Rem. Sens. GE-23(5):737–745. doi:10.1109/TGRS.1985.289392

Wu, L.K., R.K. Moore, R. Zoughi, A. Aftfi, and F.T. Ulaby. 1985b. Preliminary results on the determination of the sources of scattering from vegetation canopies at 10 GHz. Int. J. Remote Sens. 6(2):299–313. doi:10.1080/01431168508948445

Zhao, T.J., L.X. Zhang, J.C. Shi, and L.M. Jiang. 2011. A physically based statistical methodology for surface soil moisture retrieval in the Tibet Plateau using microwave vegetation indices. J. Geophys. Res. 116:D08116. doi:10.1029/2010JD015229

Zheng, G., and L.M. Moskal. 2009. Retrieving leaf area index (LAI) using remote sensing: Theories, methods and sensors. Sensors (Basel Switzerland) 9(4):2719–2745. doi:10.3390/s90402719